187. Double-Bond Shifts in [4n]Annulenes as a New Principle for Molecular Switches: First Results with Dimethyl Heptalene-1,2- and -4,5-dicarboxylates

by Anne Andrée Sophie Briquet[1]), Peter Uebelhart, and Hans-Jürgen Hansen*

Organisch-chemisches Institut der Universität, Winterthurerstrasse 190, CH–8057 Zürich

Dedicated to *Vlado Prelog* on the occasion of his 90th birthday

(15.X.96)

A new concept for molecular switches, based on thermal or photochemical double-bond shifts (DBS) in [4n]annulenes such as heptalenes or cyclooctatetraenes, is introduced (*cf. Scheme 2*). Several heptalene-1,2- and -4,5-dicarboxylates (*cf. Scheme 4*) with (*E*)-styryl and Ph groups at C(5) and C(1), or C(4) and C(2), respectively, have been investigated. Several X-ray crystal-structure analyses (*cf. Figs. 1–5*) showed that the (*E*)-styryl group occupies in the crystals an almost perfect s-*trans*-conformation with respect to the C=C bond of the (*E*)-styryl moiety and the adjacent C=C bond of the heptalene core. Supplementary ^{1}H-NOE measurements showed that the s-*trans*-conformations are also adopted in solution (*cf. Schemes 6* and *9*). Therefore, the DBS process in heptalenes (*cf. Schemes 5* and *8*) is always accompanied by a 180° torsion of the (*E*)-styryl group with respect to its adjacent C=C bond of the heptalene core. The UV/VIS spectra of the heptalene-1,2- and -4,5-dicarboxylates illustrated that it can indeed be differentiated between an 'off-state', which possesses no 'through-conjugation' of the π-donor substituent and the corresponding MeOCO group and an 'on-state' where this 'through-conjugation' is realized. The 'through-conjugation', *i.e.*, conjugative interaction *via* the involved s-*cis*-butadiene substructure of the heptalene skeleton, is indicated by a strong enhancement of the intensities of the heptalene absorption bands I and II (*cf. Tables 3–6*). The most impressive examples are the heptalene-dicarboxylates **11a**, representing the off-state, and **11b** which stands for the on-state (*cf. Fig. 8*).

1. Introduction. – It is well established that [4n]annulenes such as heptalenes ($n = 3$) or cyclooctatetraenes ($n = 2$) appear – when suitably substituted – in constitutional isomers depending on the position of their C=C bonds at the [4n] perimeter (*cf.* [1–3]). The reversible interconversion of these double-bond shifted (DBS) isomers represents π-skeletal rearrangements that may be induced thermally or photochemically (see the lit. cit. in [1–3] and especially [1] [4–6]). The energy barriers separating the twisted double-boat forms of the two DBS isomers of heptalenes and tub forms of the two DBS isomers of cyclooctatetraenes, are mainly dependent on the number and bulkiness of contiguous substituents at the two annulenes, whereby, in the case of heptalenes, the number and size of the *peri*-substituents are especially relevant. Two typical examples are shown in *Scheme 1*.

The transition state of the DBS process in heptalenes is non-planar with a maximum symmetry of D_2 of the heptalene core [1][2]), as it is demonstrated by the isoconfigurational transformation of optically active heptalenes [1] [4]. π-SCF-Force-field calculations by *Lindner* and *Flöter* are in agreement with these findings (*cf.* [3]). More recent investiga-

---

Scheme 1

1a (11.3%)　　　E = COOCH₃　　　**1b** (88.7%)ᵃ)　　　[1a]

2a (44%)　　　**2b** (56%)ᵇ)　　　[8]
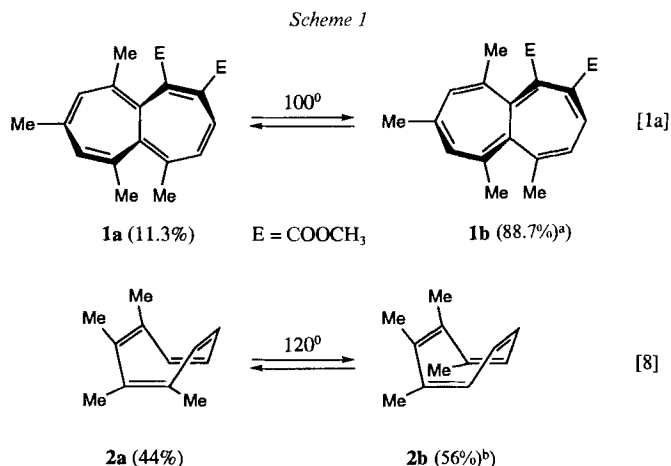
ᵃ) In tetralin, *Hafner et al.* [2] [4] determined for the DBS process **1a** → **1b** $E_a = (23.5 \bullet 0.6)$ kcal mol⁻¹ $(\Delta G_{298}^{\neq} = 26.1$ kcal mol⁻¹). Missing of the Me group at C(5) in **1a** (numbering of the heptalenes according to [7]) reduces $\Delta G_{298}^{\neq}$ of the DBS process by *ca.* 5 kcal mol⁻¹ (*cf.* [3]).

ᵇ) In (D₁₄)diglyme. The DBS process **2a** → **2b** takes place with $E_a = 28.7$ kcal mol⁻¹ $(\Delta G_{298}^{\neq} = 32.1$ kcal mol⁻¹) [8]. Missing of the Me group at C(4) in **2a** reduces E_a to 23.5 kcal mol⁻¹ $(\Delta G_{298}^{\neq} = 26.5$ kcal mol⁻¹) [9]. On the other hand, exchange of Me at C(2) and C(3) in **2a** by Ph groups let E_a increase by 6.1 kcal mol⁻¹ $(\Delta G_{298}^{\neq} = 31.2$ kcal mol⁻¹) [10].

tions of the DBS process in cyclooctatetraenes by *Paquette et al.* [6] show that it may follow also a non-planar transition state with a maximum symmetry of C_{2v} of the C_8 skeleton (*cf.* [6a]).

Nothing seems to be known about the physical mechanism of the photochemical DBS process in heptalenes and cyclooctatetraenes. Nevertheless, it has been shown that the photochemical transformation of (−)-(*P*)-**1b** leads to (−)-(*P*)-**1a** without any loss of optical purity [1a] (see also later). This indicates that the excited-state pathway must possess a similar topology as its ground state pendant³).

The thermal DBS process in heptalenes is, in general, not competed by other thermal reactions. The thermal racemization of optically active heptalenes possess distinctly higher E_a values (*e.g.*, (29.1 ± 0.4) kcal mol⁻¹ $(\Delta G_{298}^{\neq} = (31.8 \pm 0.6)$ kcal mol⁻¹)) for (−)-(*P*)-**1a** → (*MP*)-**1a**/**1b** [2] [4]) as compared with the corresponding DBS process. At higher temperatures ($\geq 200°$), heptalene-1,2-dicarboxylates may undergo a σ-skeletal rearrangement into heptalene-1,3-dicarboxylates [11] [12] (*cf.* also [2]) or disintegration to azulene-dicarboxylates [12] [13]. In contrast to heptalenes, cyclooctatetraenes, according to the D_{2d} symmetry of their [4*n*] core, are not inherently chiral, but may appear in antipodes due to their substitution pattern (*e.g.*, **2a**; *cf.* [3]). The E_a values of the racemization of optically active cyclooctatetraenes, which corresponds to a net inversion of their tub form, are normally smaller than those for the DBS process or may become quite

---

³) The photochemical DBS process in heptalenes is induced by long-wavelength irradiations ($\lambda > 400$ nm; see also later) and is linked to dissolved or otherwise oily heptalenes. In the crystalline state, heptalenes are stable, *i.e.*, show no DBS behavior (*cf.* [1a]).

similar for both envisaged reactions (*cf.* [3] [6]). As a further thermal process that may interfere with the two discussed reactions, a reversible disrotatory ring closure of cyclooctatetraenes can take place to yield bicyclo[4.2.0]octatriene derivatives (*e.g.*, **2a** is at room temperature in thermal equilibrium with a small amount of its bicyclic valence isomer, namely 1,2,7,8-tetramethylbicyclo[4.2.0]octa-2,4,7-triene [5b] [8] [14]; see also [3] [15]). Nevertheless, in both systems, the DBS process can clearly be observed separately from the other thermal reactions. In addition, heptalenes offer the advantage that the DBS process takes place here with the lowest activation energy, and only low energy irradiations ($\lambda > 360$ nm) are necessary for the photochemical variant of the DBS process.
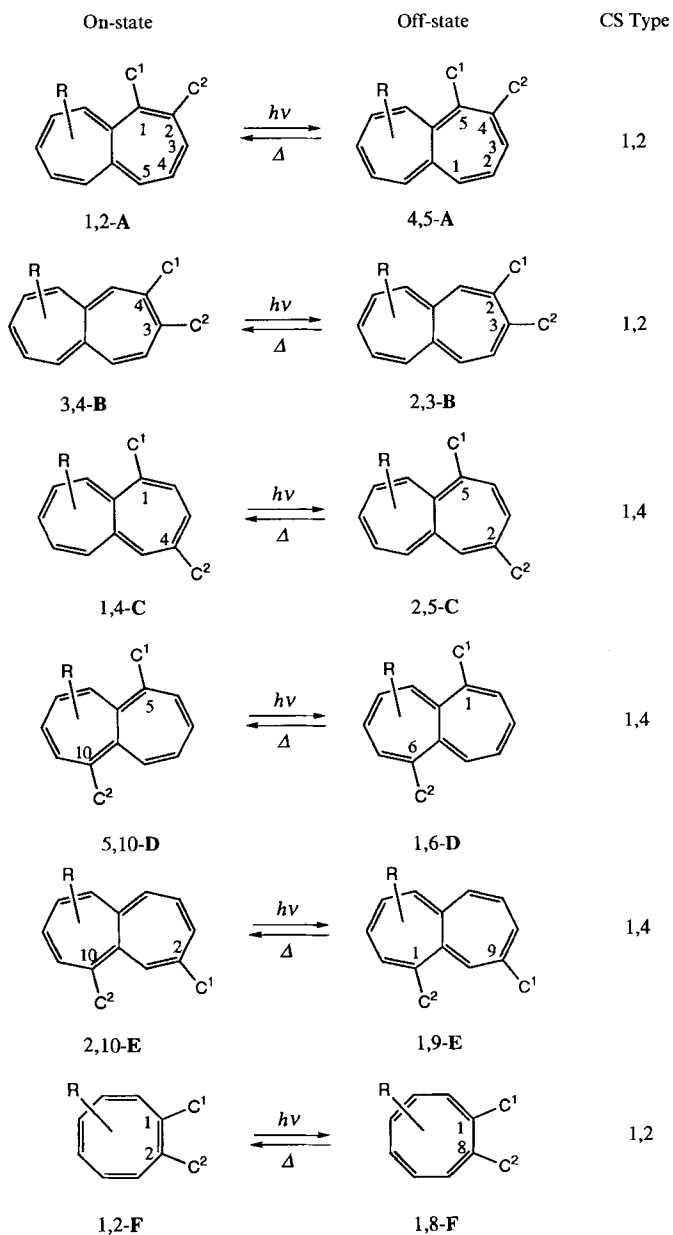
Therefore, we were interested to investigate to what extent the thermal and photochemical DBS process can be utilized as a molecular conjugative switch (CS) to turn on or off conjugation between π substituents (C^1, C^2), placed in 1,2 or 1,4 relation at the [$4n$]annulene core. The principle is depicted in *Scheme 2*. Most obvious are the possible 1,2-CS systems. However, they will have the disadvantage that the C^1 and C^2 substituents are close together in the on-state, which may lead to steric interactions between C^1 and C^2, thereby forcing one or both π substituents out of conjugation. More promising seem to be the 1,4-CS systems, 1,4-$C \rightleftarrows 2,5$-C, where conjugation between C^1 and C^2 can be realized *via* an s-*cis*-butadiene substructure. The torsion angles of such s-*cis*-butadiene substructures in heptalenes, carrying three or four *peri*-substituents (one being MeOCO, the others Me), vary in the narrow range of 31–34.5°, and the C_2-symmetric 1,3,5,6,8,10-hexamethylheptalene (**3**) [16][4]) may be taken as a model compound (*cf. Scheme 3*; see also later). This means that conjugation *via* the s-*cis*-butadiene subunits will not be reduced by more than a fifth (*cf. e.g.* [18]), assuming that C^1 and C^2 are in an optimal conformation (*i.e.*, Θ near 0 or 180°) with respect to 'their' heptalene C=C bonds in the on-state. The systematically possible 1,4-CS arrangement 5,10-$D \rightleftarrows 1,6$-D and 2,10-$E \rightleftarrows 1,9$-E will not be very effective as conjugative switches due to the unfavorable Θ_{av} of the involved s-*trans*-butadiene subunits which vary in the range of 112–122° (**D**-type) and 114–124° (**E**-type) for heptalenes bearing three or four *peri*-substituents (*cf. Scheme 3*) and will reduce conjugation by up to 60%. The situation is similar to higher substituted cyclooctatetraenes where X-ray crystal diffraction analyses reveal that the average torsion angles between the ethylene subunits fluctuate in the range of 64 to 69° (*cf. e.g.* [21])[5]). Therefore, cyclooctatetraenes will only be useful as switches in the 1,2-CS setting (*cf. Scheme 3*).

In this work, we will report on the X-ray crystal structure, the solution structure, and the UV/VIS behavior of dimethyl heptalene-1,2- and -4,5-dicarboxylates, substituted with phenyl and (*E*)-2-phenylethenyl groups at C(4) or C(5), and at C(1) and C(2), respectively (see *Scheme 4*). This means that C^1 is represented by the π-acceptor substituent MeOCO and C^2 by the π-donor substituents 4-R—C_6H_4 (R=H, MeO) and (*E*)-4-R—C_6H_4CH=CH (R=H, Cl, MeO). The other heptalene-dicarboxylates (**5a/b**,

---

[4]) Indeed, the twisting of the heptalene skeleton as expressed in Θ (s-*cis*-butadiene) is sensitive to the number of *peri*-substituents: dimethyl heptalene-3,8-dicarboxylate, possessing no *peri*-substituents, exhibits Θ_{av}(s-*cis*-butadiene) = 18.5° [19]. However, already one *peri*-substituent, as in dimethyl heptalene-4,5-dicarboxylate, pushes Θ_{av}(s-*cis*-butadiene) up to 31.5° [20], *i.e.*, already close to Θ_{av}(s-*cis*-butadiene) of heptalenes carrying three or four *peri*-substituents (*vide supra*).
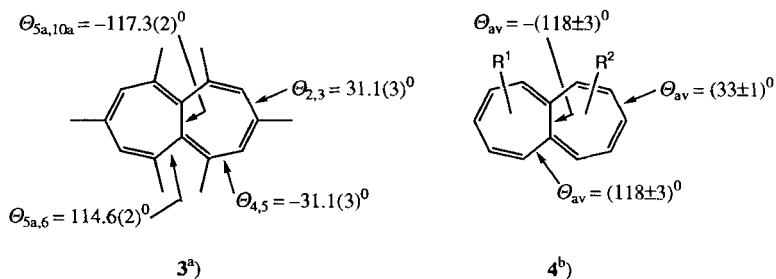
[5]) If we take cyclooctatetraene itself with the flattest tub conformation into account [22], the Θ_{av} range is extended to 58 to 69°.

Scheme 2

On-state	Off-state	CS Type
1,2-A	4,5-A	1,2
3,4-B	2,3-B	1,2
1,4-C	2,5-C	1,4
5,10-D	1,6-D	1,4
2,10-E	1,9-E	1,4
1,2-F	1,8-F	1,2

[a]) C^1,C^2: π substituents, capable of conjugation; R = nonconjugative substituents (e.g. alkyl groups) which moderate via their steric interactions E_a of the thermal DBS process; CS: conjugative switch in local 1,2 (1,2-CS) or 1,4 relation (1,4-CS) at the [4n] perimeter; on-state: C^1 and C^2 are in conjugation via the ethylene or s-cis- or s-trans-buta-1,3-diene substructure of the [4n]annulene core; off-state: interruption of the direct conjugation of C^1 and C^2.

Scheme 3

$\Theta_{5a,10a} = -117.3(2)^0$

$\Theta_{2,3} = 31.1(3)^0$

$\Theta_{5a,6} = 114.6(2)^0$

$\Theta_{4,5} = -31.1(3)^0$

$\Theta_{av} = -(118\pm3)^0$

R^1 R^2

$\Theta_{av} = (33\pm1)^0$

$\Theta_{av} = (118\pm3)^0$

3[a])   **4**[b])

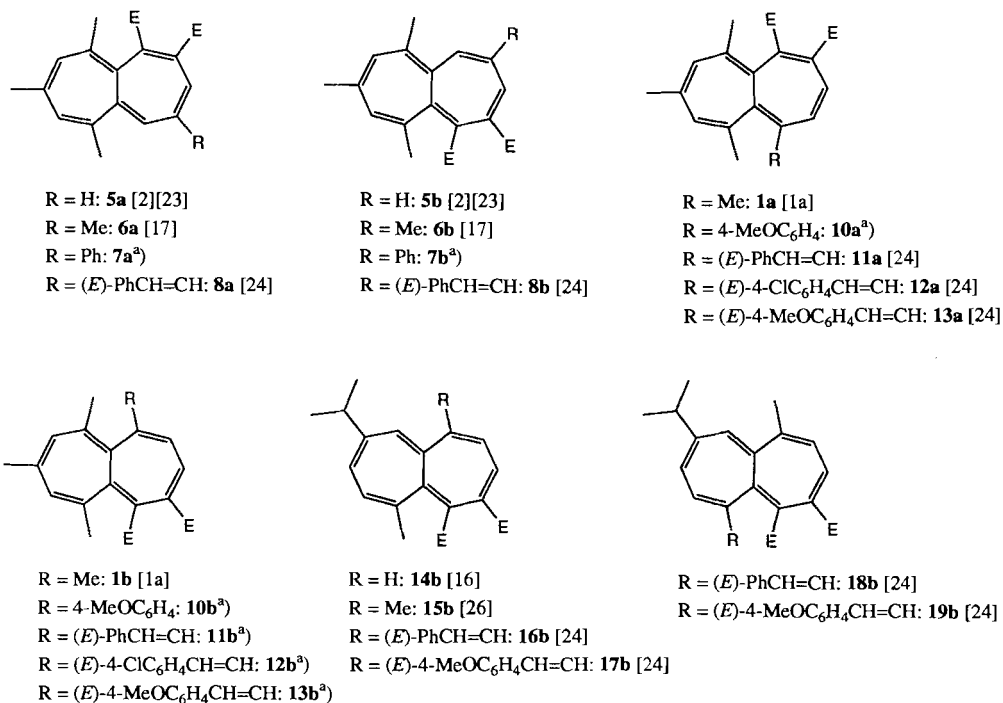[a]) $\Theta_{n,m}$ are taken from an X-ray crystal-diffraction analysis at 173(1) K [16].

[b]) $\Theta_{av} = 0.25 \cdot \Sigma\Theta_{n,m}$ from a number of X-ray crystal-diffraction analyses of heptalenes carrying three or four *peri*-substituents (Me, MeOCO). R^1, R^2 = additional substituents (Me, i-Pr, or *t*-Bu) (*cf.* [1] [11] [17]).

6a/b, **9a/b** as well as **14b** and **15b**) served together with 1,3,5,6,8,10- (**3**) [16] as well as 1,2,5,6,8,10- and 1,4,5,6,8,10-hexamethylheptalene (**9a** and **9b**) [27] [28] as reference compounds for UV/VIS spectroscopy[6]).

Scheme 4

R = H: **5a** [2][23]
R = Me: **6a** [17]
R = Ph: **7a**[a])
R = (*E*)-PhCH=CH: **8a** [24]

R = H: **5b** [2][23]
R = Me: **6b** [17]
R = Ph: **7b**[a])
R = (*E*)-PhCH=CH: **8b** [24]

R = Me: **1a** [1a]
R = 4-MeOC$_6$H$_4$: **10a**[a])
R = (*E*)-PhCH=CH: **11a** [24]
R = (*E*)-4-ClC$_6$H$_4$CH=CH: **12a** [24]
R = (*E*)-4-MeOC$_6$H$_4$CH=CH: **13a** [24]

R = Me: **1b** [1a]
R = 4-MeOC$_6$H$_4$: **10b**[a])
R = (*E*)-PhCH=CH: **11b**[a])
R = (*E*)-4-ClC$_6$H$_4$CH=CH: **12b**[a])
R = (*E*)-4-MeOC$_6$H$_4$CH=CH: **13b**[a])

R = H: **14b** [16]
R = Me: **15b** [26]
R = (*E*)-PhCH=CH: **16b** [24]
R = (*E*)-4-MeOC$_6$H$_4$CH=CH: **17b** [24]

R = (*E*)-PhCH=CH: **18b** [24]
R = (*E*)-4-MeOC$_6$H$_4$CH=CH: **19b** [24]

[a]) This work; see also *Sect. 2* and *3*.

[6])   See [29] and lit. cited therein for molecular switches and optical storage systems.

2. Structure Determinations. 2.1. *Dimethyl 6,8,10-Trimethyl-2-[(E)-2-phenyl-ethenyl]heptalene-4,5-dicarboxylate* (**8b**) *and Its DBS Isomer* **8a**. At room temperature, in solution, both DBS isomers are in thermal equilibrium (*Scheme 5*). However, from hexane/Et$_2$O, on cooling, only **8b** crystallizes in orange-red plates. The X-ray crystal structure of these plates is shown in *Fig. 1*. Important structural data of the crystal structure are collected in *Table 1*. As can be recognized, the (*E*)-styryl substituent at C(2)
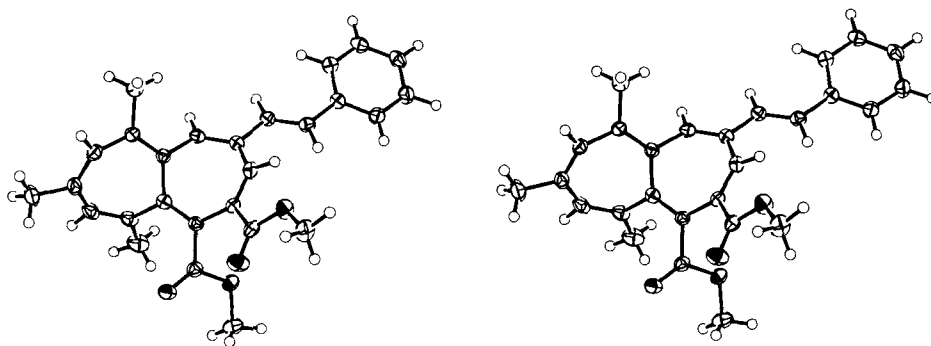
Fig. 1. *Stereoscopic view of the X-ray crystal structure*
of dimethyl 6,8,10-trimethyl-2-[(E)-2-phenylethenyl]heptalene-4,5-dicarboxylate (**8b**)

Table 1. *Characteristic X-Ray Crystallographic Data of the Dimethyl Heptalene-4,5-dicarboxylates*

Parameter	8b	7b	11b	10b	18b
$d_{av}(\sigma)^a$ [Å]	1.467(18)	1.468(15)	1.468(19)	1.470(19)	1.459(25)
$d(C(5a)-C(10a))$ [Å]	1.490(3)	1.483(2)	1.482(2)	1.482(2)	1.475(2)
$d_{av}(\pi)^b$ [Å]	1.351(4)	1.355(4)	1.354(6)	1.353(5)	1.345(7)
$\Sigma\vartheta(1)^c$ [°]	856.3(3)	859.6(1)	857.5(2)	858.0(1)	861.2(2)
$\Sigma\vartheta(2)$ [°]	862.7(3)	855.5(1)	853.4(2)	852.4(1)	856.8(2)
$\vartheta_{av}^{d)e}$ [°]	123(4)	122.5(5.0)	122(5)	122(5)	123(5)
$\Theta(1)^f$ [°]	−123.9(3)	−123.6(1)	−114.4(2)	−113.7(1)	−121.4(2)
$\Theta_{av}(2)$ [°]	127(1)	122(2)	118.5(2.0)	−119(1)	122(2)
$\Theta_{av}(3)$ [°]	34(3)	34(2)	33(3)	33(2)	32(1)
$\Theta(4)$ [°]	−175.7(2)	–	−179.3(2)	–	−178.8(2)
$\Theta(5)$ [°]	11.6(4)	31.2(2)	17.6(3)	25.4(2)	20.5(3)
	−169.6(3)	−150.0(1)	−160.5(2)	−154.6(1)	−161.2(2)

^a)　Average values of the six σ bonds in the heptalene perimeter. In parantheses for these and the other parameters are given the standard deviations.
^b)　Average values of the six π bonds in the heptalene perimeter.
^c)　$\Sigma\vartheta(1)$: sum of the bond angles of the seven-membered ring carrying the two MeOCO groups; sum of the angles of a seven-membered polygon = 900°. $\Sigma\vartheta(2)$: sum of the bond angles of the second seven-membered ring.
^d)　ϑ_{av}: average values of all 14 bond angles of the two seven-membered rings.
^e)　The comparably large standard deviations of ϑ_{av} are due to the bond angles at the central σ-bond which have to compensate much of the strain of the heptalene skeleton. Their average values over all five heptalenes amount to (113.5 ± 1.5)° for the 'geminal' bond angles (see also Table 3 in [17]) and (119.8 ± 1.0)° for the olefinic bond angles. If these angles are neglected, ϑ_{av} increases to (125 ± 2)° for all five heptalenes.
^f)　$\Theta(1) = \Theta$(s-*trans*-butadiene) of the central substructure. $\Theta_{av}(2)$: average value of the two s-*trans*-butadiene subunits of the heptalene perimeter. $\Theta_{av}(3)$: average value of the four s-*cis*-butadiene subunits of the heptalene perimeter. $\Theta(4) = \Theta$(s-*trans*-butadiene) of the C(1')=C(2') bond of the (*E*)-styryl substituent at the corresponding C=C bond at the heptalene core. $\Theta(5)$: tilt angles of the Ph group at C(2') of the (*E*)-styryl group or at the corresponding C=C bond at the heptalene core.

adopts in the crystals a nearly perfect s-*trans*-conformation with respect to the heptalene C(1)=C(2) bond, *i.e.*, Θ(C(1)=C(2)–C(1')=C(2')) amounts to 176° (*Table 1*) and Θ_{av}(s-*cis*-butadiene) of the heptalene perimeter falls with $(34 \pm 3)°$ well within the general range (*cf. Scheme 3*). The torsion angle Θ(C(10)=C(10a)–C(1)=C(2)) is 126.0(3)°, indicating that there is only a weak conjugative interaction of the (*E*)-PhCH=CH–C(2)=C(1) fragment with the heptalene π core. On the other hand, the torsion angles of the ethenyl group with the phenyl moiety ($\Theta = 11.6(4)°$ and –169.6(3)°, resp.) indicate again an excellent planar interaction of the two π systems.

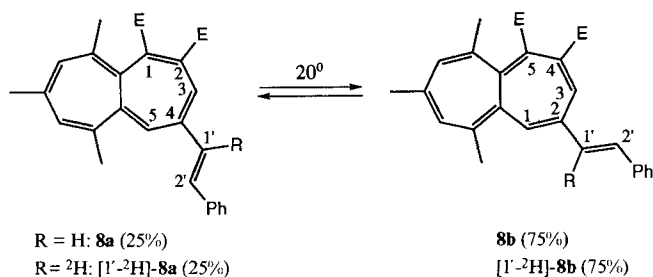The conformational situation in the crystals is also found in solution (CDCl₃ and C_6D_6) at room temperature as evidenced by corresponding ¹H-NOE measurements of **8b** as well as of **8a**. Unfortunately, the ¹H-NMR spectrum of **8a** showed for the essential *AB* system of H–C(1') and H–C(2'), also at 600 MHz, almost no resolution in CDCl₃ ($\delta = 6.80$ ppm; $\Delta v = < 1$ Hz) and only a slight resolution in C_6D_6 (δ(H–C(1')) = 6.61 and δ(H–C(2')) = 6.64 ppm; $\Delta v = 9.8$ Hz). The DBS isomer **8b** exhibited certainly a clearly separated *AB* system in CDCl₃ (δ(H–C(1')) = 6.77 and δ(H–C(2')) = 6.93 ppm) but no resolution of the chemical shift of these H-atoms in C_6D_6 ($\delta = 6.77$ ppm; $\Delta v = < 1$ Hz). Since these circumstances did not allow an unequivocal assignment of the chemical shifts of H–C(1') and H–C(2'), we synthesized the corresponding compounds [1'-²H]-**8a**/[1'-²H]-**8b**, carrying specifically a ²H-atom at C(1') (*cf. Scheme 5*)[7]. As a result, [1'-²H]-**8a** showed in the ¹H-NMR spectrum at 600 MHz (C_6D_6) only a *s* at 6.64 ppm, and [1'-²H]-**8b**, in turn, an *s* at 6.93 ppm (CDCl₃) leading to the above mentioned assignments. The results of the ¹H-NOE measurements with **8a** and **8b** and their isotopomers [1'-²H]-**8a**/[1'-²H]-**8b** in both solvents are summarized in *Scheme 6*. The strong (s) effects that are observed between H–C(1') and H–C(3) as well as between H–C(2') and H–C(5) are in agreement with a preferred s-*trans*-conformation around the C(1')=C(2') bond in **8a**. The DBS isomer **8b** shows in solution the same behavior according to the strong effects that are observed between H–C(1') and H–C(1) as well as between H–C(2') and H–C(3). The additional effects of strong and medium (m) intensity which are observed between H–C(1') and H–C(2'), and the two H_o-atoms of the Ph group in both isomers indicate that the torsion angles between C(1')=C(2') and the Ph group, in average, are also close to 0° and 180°, respectively. On the other hand, the irradiation of H–C(2') in [1'-²H]-**8a** and [1'-²H]-**8b** induced also weak effects on H–C(3) and H–C(5), respectively. The integration of the induced signals at H–C(5)/H–C(3) of [1'-²H]-**8a** as well as at H–C(1)/H–C(3) of [1'-²H]-**8b** gave ratios of 7.3:1 and > 12:1, respectively, if we assume that the rotation around the C(1')–C(2) bond in **8b** is fast[8]), and

---

[7]) The synthesis was realized in the established manner for **8a**/**8b** [24], starting with methyl 4,6,8-trimethylazulene-2-carboxylate [30] which was reduced with LiAl[²H₄] in Et₂O and then dehydrogenated with MnO₂ in CH₂Cl₂ to the corresponding azulene-2-[²H]carbaldehyde [31] (for details, see *Exper. Part*).
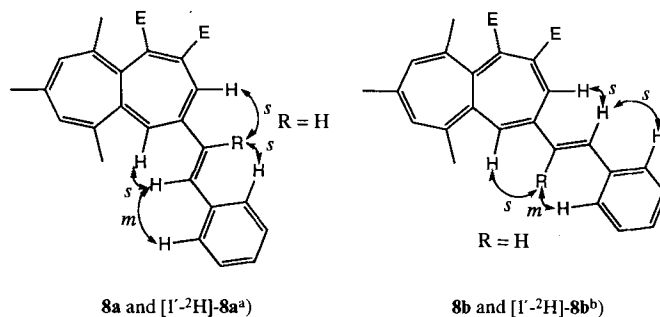
[8]) Experimental results and calculations of the internal barrier of rotation in substituted ethylenes and benzenes (*cf.* [32] and lit. cited there) as well as in *trans*-stilbenes (*cf.* [33] and lit. cited there) are in excellent agreement. They amount to 3 kcal mol⁻¹ for styrene and 6 kcal mol⁻¹ for buta-1,3-diene. The optimized geometry for styrene is not planar with an equilibrium torsion angle of 19°. Similarly, the s-*cis*-conformation of buta-1,3-diene is not planar. The optimized *gauche*-conformation is by *ca.* 1 kcal mol⁻¹ more stable than the planar s-*cis*-arrangement. Electron-diffraction experiments at 200° yielded for *trans*-stilbene dihedral angles between the Ph ring and the central ethylene bond of $(31 \pm 5)°$ [34]. Calculations of *Lhost* and *Brédas* [33] showed that the corresponding potential-energy curves are very flat in *trans*-stilbene for torsion angles between –30 and +30°.

the transfer of magnetization is the same in the conformers, the observed weak ¹H-NOE would indicate that *ca.* 10 % of the corresponding s-*cis*-conformations[8]) are in thermal equilibrium with their s-*trans*-conformations at room temperature.

Scheme 5

R = H: **8a** (25%)
R = ²H: [1′-²H]-**8a** (25%)

8b (75%)
[1′-²H]-**8b** (75%)

Scheme 6

8a and [1′-²H]-**8a**[a])

8b and [1′-²H]-**8b**[b])

[a]) s = strong, m = medium. Irradiation of H–C(2′) at 6.80 ppm (CDCl₃) in [1′-²H]-**8a** gave a weak (w) ¹H-NOE also on H–C(3) at 6.57 ppm. Integration of the ¹H-NOE on H–C(3) and H–C(5) revealed a ratio of *ca.* 7.3:1.
[b]) Irradiation of H–C(2′) at 6.76 ppm (CDCl₃) in [1′-²H]-**8b** resulted in the indicated strong ¹H-NOE on H–C(3) at 7.93 ppm. However, a very weak ¹H-NOE was also observed on H–C(1) at 6.15 ppm with an estimated ratio of integration of > 12:1.

The experimental results in solution reveal that the DBS process in **8a** and **8b** is also accompanied by a change in the spatial arrangement of the (*E*)-styryl side chain in a way that it follows the cyclic DBS process in the heptalenes by adopting always the energetically most favorable s-*trans*-conformation with respect to its heptalene C=C bond (*cf. Schemes 5* and *6*).

    2.2. *Dimethyl 6,8,10-Trimethyl-2-phenylheptalene-4,5-dicarboxylate* (**7b**) *and Its DBS Isomer* **7a**. The synthesis was realized by the thermal reaction of 4,6,8-trimethyl-2-phenyl-azulene [35] with dimethyl acetylenedicarboxylate (see *Exper. Part*). Both isomers, **7a** and **7b**, form at room temperature a thermal equilibrium mixture consisting of 23 % of **7a** and **7b** (*Scheme 7*). In hexane/Et₂O, **7b** crystallizes from this mixture in orange prisms. The X-ray crystal structure of these prisms is shown in *Fig. 2*. Relevant structural data from this analysis are collected in *Table 1*. The Ph ring is slightly twisted with respect to the plane of the C(1)=C(2) bond of the heptalene core. The corresponding torsion angles

amount to $-150.0(1)°$ and $31.2(2)°$, respectively. They are still in the range of the flat potential curve for stilbenes (cf. [33]). The s-cis-butadiene subunits of the heptalene skeleton show $\Theta_{av} = (34 \pm 2)°$, i.e., just the same value as the ethenyl homologue **8b** (Table 1). The corresponding Θ_{av}(s-trans-butadiene) value amount to $(122 \pm 2)°$, again, as expected, close to that of **8b** $(\Theta_{av}$(s-trans-butadiene) $= (127 \pm 1)°)$. It also demonstrates that conjugation is mainly restricted to the corresponding 2-phenylethenyl subunit (Ph−C(2)=C(1)) in **7b**. The nearly identical thermal equilibrium composition of **8a**/**8b** and **7a**/**7b** in solution (Schemes 5 and 7) is a clear indication that the behavior of **7a** and **7b** in solution must be quite similar to that of **8a** and **8b**. This view is fully supported by the UV/VIS spectra of the DBS isomers of both heptalenes (see Sect. 2.3).
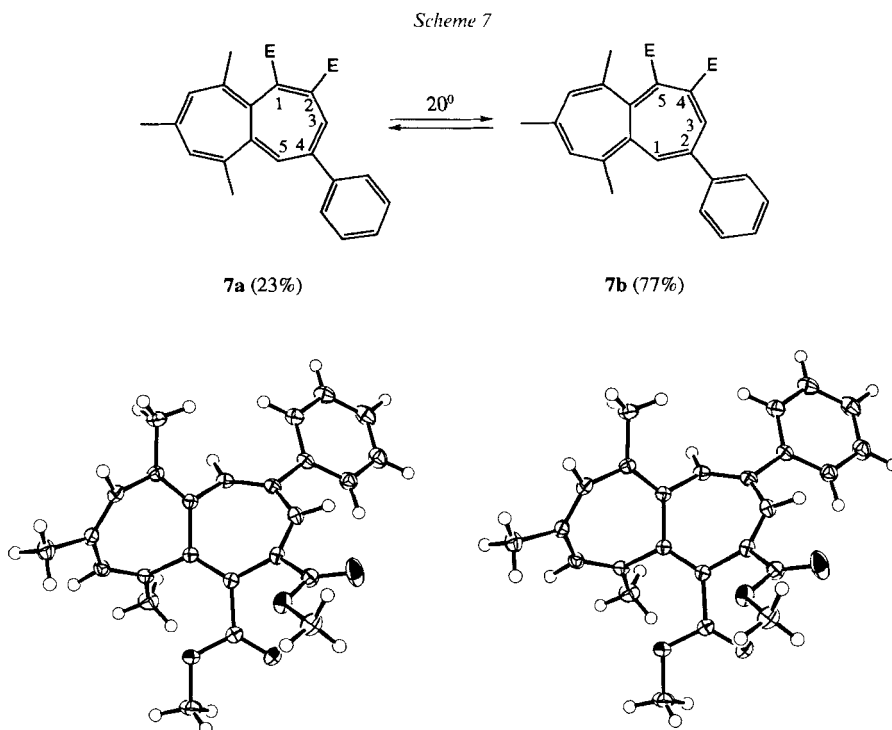
Scheme 7

7a (23%)　　　　　　　　　　　　**7b** (77%)

Fig. 2. Stereoscopic view of the X-ray crystal structure
of dimethyl 6,8,10-trimethyl-2-phenylheptalene-4,5-dicarboxylate (**7b**)

2.3. *Dimethyl 6,8,10-Trimethyl-1-[(E)-2-phenylethenyl]heptalene-4,5-dicarboxylate* (**11b**) *and Its DBS Isomer* **11a**. The catalyzed reaction of 4,6,8-trimethyl-1-phenylazulene with dimethyl acetylenedicarboxylate led – beside other products – only to the formation of **11b** [24] which crystallized in orange plates from hexane/Et₂O. Indeed, heating of **11b** in toluene did not give its DBS isomer **11a** in detectable amounts. On the other hand, irradiation of **11b** in hexane with 366-nm light established readily a photostationary state of **11b** and **11a** which consisted of 68% of **11b** and 32% of **11a** (Scheme 8). The photo-equilibrium could be further shifted in favor of **11a** when the irradiation was performed with light of $\lambda > 400$ nm (see Scheme 8).

Scheme 8
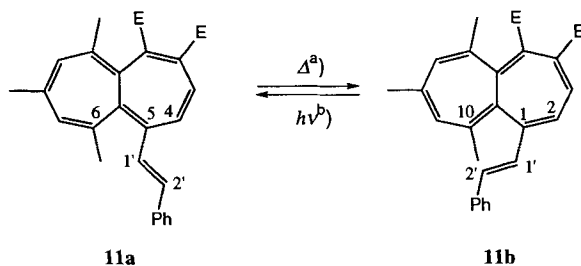
11a　　　　　　　　　　**11b**

The results of the X-ray diffraction analysis of the orange plates of **11b** are displayed in *Fig. 3* and collected in *Table 1*. There is found again a perfect s-*trans*-conformation of the styryl group and the C(1)=C(2) bond of the heptalene core ($\Theta(C(2')=C(1')-C(1)=C(2)) = 179.3(2)°$). The Ph group is, as in the other cases, slightly twisted with respect to the plane of the ethenyl group ($\Theta = -161.2(2)°$ and 20.5(3)°). The Me group at C(10) does not interfere sterically with the external ethenyl bond, since it is well placed beneath this bond^9). Θ_{av}(s-*cis*-butadiene) of the heptalene skeleton fits with $(32 \pm 3)°$ also well into the general range (*Scheme 3*). The specific torsion angle $\Theta(C(1)=C(2)-C(3)=C(4)) = 29.6(3)°$ shows that there should exist a 'through-conjugation' in the molecule between the (*E*)-styryl group at C(1) and the MeOCO group at C(4)^{10}) what is indeed found in the UV/VIS spectrum of **11b** (see *Chapt. 3*). Θ_{av}(s-*trans*-butadiene) = $(118.5 \pm 0.2)°$ is quite low, however, still within the range of other heptalenes carrying four *peri*-substituents (*cf. Scheme 3*). It may be taken as the lower limit for Θ_{av} of the DBS isomer **11a** where no X-ray structure is available. It indicates that the conjugative coupling between the structural segment C(2')=C(1')−C(5)=C(5a) of **11a** and the adjacent linearly placed C=C bond of the heptalene core (C(6)=C(7)) will again be very small^{11}).

---

^{9})　This spatial relation is also documented in the chemical shift of Me−C(10) (δ(CHCl$_3$) = 1.65 ppm) as compared to that of Me−C(10) of **8b** (δ(CDCl$_3$) = 1.81 ppm). The high-field shift by −0.16 ppm of Me−C(10) of **11b** is the result of the shielding effect of the optimally placed (*E*)-styryl group at C(1).

^{10})　The 'through-conjugation' in the crystals of **11b** holds also for the MeOCO group at C(4) which occupies an s-*cis*-conformation with respect to the C(3)=C(4) bond with $\Theta(O=C-C(4)=C(3)) = -13.2(3)°$. An additional argument for the 'through-conjugation' in **11b** can also be found in the stretching frequencies of the C=O groups in the IR spectrum. Heptalene-dicarboxylate **11b** and its methyl analogue **1a** [1a] (*cf. Scheme 4*) crystallize both in the space group $P2_1/c$ and show in their IR spectra (KBr) two ν(C=O) bands at 1720 and 1710 cm^{-1} for **11b** (see *Exper. Part*), and at 1737 and 1720 cm^{-1} for **1b** [25]. The displacement by 10–17 cm^{-1} to lower frequencies is quite generally found for the effect of conjugation on ester groups.

^{11})　This should also be true for C(10)=C(10a), since the central torsion angle of **11a** will be close to that of **11b** ($\Theta = -121.4(2)°$; see also *Scheme 3*).
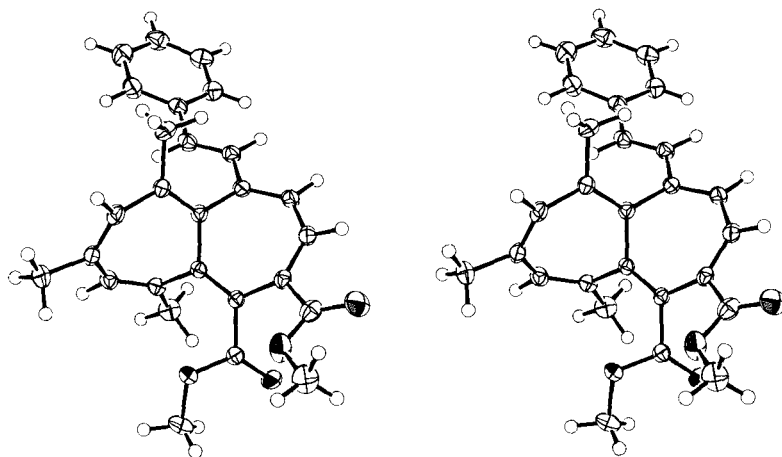
Fig. 3. *Stereoscopic view of the X-ray crystal structure*
of dimethyl 6,8,10-trimethyl-1-[(E)-2-phenylethenyl]heptalene-4,5-dicarboxylate (**11b**)

The results of the ^{1}H-NOE measurements of **11a** and **11b** are summarized in *Scheme 9*. They show that, of both DBS forms, only the s-*trans*-conformation is occupied within the limits of detection. The weak ^{1}H-NOE that is observed at H−C(1′) of **11b** when Me−C(10) is irradiated cannot be attributed to a corresponding s-*cis*-conformation around the C(1)−C(1′) bond, because no corresponding ^{1}H-NOE at H−C(2′) is recognizable by irradiation of H−C(2). Indeed, the situation of Me−C(10) beneath the C(1′)=C(2′) bond brings Me−C(10) also close to H−C(2′) in the perferred s-*trans*-conformation around the C(1)−C(1′) bond of **11b** (see also *Exper. Part*). In total, the ^{1}H-NOE measurements show that the DBS process at the heptalene skeleton is accompanied – as in the case of **8a**⇌**8b** – by a reorientation of the (*E*)-styryl substituent in space, in a way that its s-*trans*-arrangement follows the position of the conjugated C=C bond of the heptalene skeleton (*cf. Scheme 8*).

Scheme 9[a])

11a   **11b**
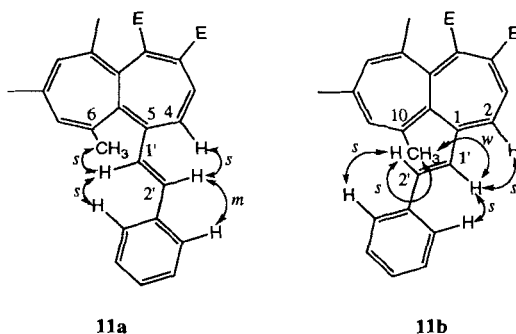
[a]) ^{1}H-NOE Measurements at 400 MHz (CDCl$_3$); s = strong, m = medium, w = weak; for details see *Exper. Part*.

The very similar chemical shifts of the four derivatives of **11a** and **11b**, namely of the Cl derivatives **12a**/**12b** and the MeO derivatives **13a**/**13b**, manifest that they all prefer the s-*trans*-conformation between the relevant conjugated heptalene C=C bond and the substituted (*E*)-styryl group (see *Exper. Part*). The DBS process in **12b** and **13b** could only be induced photochemically (see *Scheme 10*). Thermally, **12a** and **13a** were completely transformed into **12b** and **13b**, respectively.

Scheme 10

80°
366 nm

R = Cl: **12a** (20%)[a]   **12b** (80%)
R = MeO: **13a** (13%)[a]   **13b** (87%)

[a]) Amounts in the photostationary state in hexane after irradiation with 366-nm light of a fluorescence tube. The thermal reaction in toluene leads quantitatively to **12b** and **13b**, respectively.

2.4. Dimethyl 1-(4-Methoxyphenyl)-6,8,10-trimethylheptalene-4,5-dicarboxylate (10b) *and Its DBS Isomer* 10a. Compound **10b** was obtained in small yield beside other products – mainly dimethyl 4,6,8-trimethylazulene-1,2-dicarboxylate (see *Exper. Part*) – from the [RuH$_2$(PPh$_3$)$_4$]-catalyzed reaction (*cf.* [36] [37]) of 1-(4-methoxyphenyl)-4,6,8-trimethylazulene [35] and dimethyl acetylenedicarboxylate in MeCN. It crystallized from hexane/Et$_2$O in orange prisms which gave a good X-ray diffraction pattern for the crystal structure analysis (*Fig. 4*). The structural situation is quite similar to that of the Ph-sub-

Fig. 4. *Stereoscopic view of the X-ray crystal structure
of dimethyl 1-(4-methoxyphenyl)-6,8,10-trimethylheptalene-4,5-dicarboxylate* (**10b**)

stituted heptalene-dicarboxylate **7b**. The 4-methoxyphenyl ring is slightly tilted with respect to the relevant C(1)=C(2) bond of the heptalene skeleton (Θ (4-MeOC$_6$H$_4$–C(1)=C(2)) = 25.4(2)° and −154.6(1)°, resp.; *cf. Table 1*). Θ_{av}(s-*cis*-butadiene) amounts to (33 ± 2) and the relevant Θ (C(1)=C(2)–C(3)=C(4)) to −30.9(2)°, *i.e.*, the crystal structure allows a good 'through-conjugation' of the 4-methoxyphenyl group at C(1), and the MeOCO substituent at C(4) (Θ (O=C–C(4)=C(3)) = −156.2(1)°) is also still in the range of a high degree of conjugation). The torsion angles of the peripheral s-*trans*-butadiene subunits of the heptalene core are again with Θ_{av} = 119.2(1)° full in the range of other heptalenedicarboxylates (*cf. Scheme 3*).

Irradiation of a solution of **10b** in hexane with 366-nm light led rapidly to a photostationary state with its DBS isomer **10a** (*Scheme 11*).

Scheme 11

366 nm^a)

hexane

10a (38%)　　　　　　　　　　　　**10b** (62%)
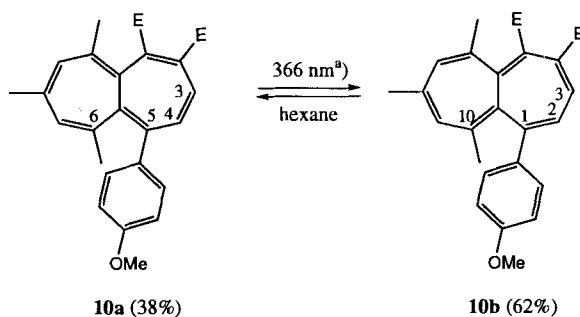
^{a}) Irradiation with 366-nm light of a fluorescence tube.

The DBS process was clearly indicated by the increased coupling constant ^3J(H–C(2),H–C(3)) = 11.9 Hz with respect to that of the starting material **10b** (^3J(H–C(3),H–C(4))) = 6.3 Hz). That the 4-methoxyphenyl ring in **10a** has slightly changed its spatial relation to the Me group at C(10) is indicated by the chemical-shift difference of this group (δ = 1.64 ppm in comparison to **10b** (δ(Me–C(6)) = 1.46 ppm)).

2.5. Dimethyl 9-Isopropyl-1-methyl-6-[(E)-2-phenylethenyl]heptalene-4,5-dicarboxylate (**18b**). The compound is formed in the purely thermal as well as in the [RuH$_2$(PPh$_3$)$_4$]-catalyzed reaction (*cf.* [36] [37]) of 9-isopropyl-1-methyl-8-[(*E*)-2-phenylethenyl]azulene with dimethyl acetylenedicarboxylate [24]. It crystallized in orange prisms from hexane/Et$_2$O. To complete our picture of (*E*)-styryl-substituted heptalene-dicarboxylates, **16b** was also subjected to an X-ray crystal-structure analysis. The stereoscopic view of the crystal structure of **16b** is displayed in *Fig. 5*. We recognize again that the (*E*)-styryl substituent at C(6) occupies an almost perfect s-*trans*-conformation with respect to the C(6)=C(7) bond of the heptalene core (Θ (C(2')=C(1')–C(6)=C(7)) = 178.8(2)°; *cf. Table 1*). The tilt of the Ph ring with respect to the plane of the C(2')=C(1') bond is also in the normal range (Θ (Ph–C(2')=C(1')) = −161.2(2)° and 20.5(3)°). Θ_{av}(s-*cis*-butadiene) = (32 ± 1)° as well as Θ_{av}(s-*trans*-butadiene) = (122 ± 2)° fit also in the normal range (*cf. Scheme 3*).
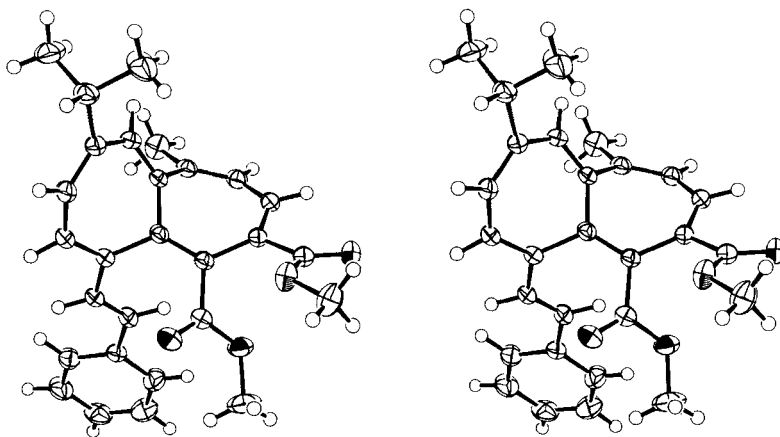
Fig. 5. *Stereoscopic view of the X-ray crystal structure*
of dimethyl 9-isopropyl-1-methyl-6-[(E)-2-phenylethenyl]heptalene-4,5-dicarboxylate (**16b**)

The nearly ideal s-*trans*-conformation of the structural segment (E)-PhCH=
CH–C(6)=C(7) places the MeOCO group at C(5) closely beneath the Ph ring (see also
Scheme 12). This structural feature can also be recognized in solution. All heptalene-4,5-
dicarboxylates bearing a Me group at C(6) exhibit in their ^{1}H-NMR spectra (CDCl$_3$ or
CCl$_4$) for the two MeOCO groups two *s* of very similar chemical shifts close to 3.70 ppm
(*e.g.* **1a**: 3.69/3.71 ppm [1a]; **11b**: 3.75/3.71 ppm [24]; **15b**: 3.63/3.60 ppm (CCl$_4$) [26][12];
3.71/3.71 ppm (CDCl$_3$) [38]). This situation is changed in the case of **16b** and its 4-MeO
derivative **17b**. Both compounds exhibit for their MeOCO groups two *s* at 3.73 and
3.50 ppm. The observed shift difference of *ca.* 0.2 ppm for MeOCO–C(5) of **18b** and **19b**

Scheme 12

R = H: **18b**
R = MeO: **19b**

___
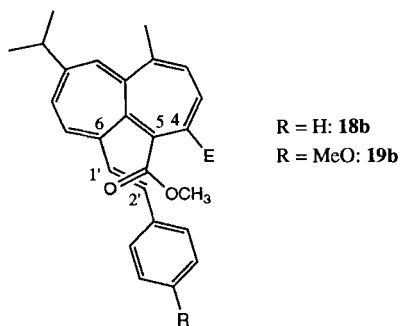
[12]　The diester **15b** with a [^{2}H$_3$]methoxycarbonyl group at C(5) shows in the ^{1}H-NMR spectrum (CCl$_4$) for
MeOCO–C(4) a *s* at 3.63 ppm [11]. It seems, therefore, that all considered dimethyl heptalene-4,5-dicarboxy-
lates show δ(MeOCO–C(4)) > δ(MeOCO–C(5)) in CCl$_4$ or CDCl$_3$.

can be interpreted as a shielding effect of the Ph group at C(2′) due to the preferred s-*trans*-conformation of the (*E*)-styryl group at C(6) also in solution.

3. UV/VIS Spectra of the Dimethyl Heptalene-1,2- and -4,5-dicarboxylates. – 3.1. *Basal Structures.* The UV/VIS spectrum of heptalene itself has already been reported by *Dauben* and *Bertelli* [39] who were the first to synthesize the parent molecule. Later, the spectrum was confirmed by *Vogel et al.* [40] [41] who obtained the labile heptalene in the crystalline state (brown crystals) and also synthesized the rigidly bent 1,7-methano-[12]annulene [42]. The spectrum of heptalene is characterized by two broad absorption bands in the short-wavelength region (cyclohexane: 256 and 352 nm with $\varepsilon = 21400$ and 4140, resp.) followed by an extremely long tailing up to above 650 nm. 1,7-Methano-[12]annulene exhibits a similar spectroscopic behavior (see *e.g.* [41]) in that it also possesses a strong absorption band around 252 nm (cyclohexane), however, now followed by a shoulder at *ca.* 300 nm and a broad absorption around 425 nm with its spur reaching down to 600 nm. The latter spectroscopic behavior is more or less reflected in the UV/VIS spectra of all simply substituted heptalenes with C_2 symmetry of their inherent chiral skeleton. As an example, *Fig. 6* shows the UV/VIS spectrum of 1,3,5,6,8,10-hexamethylheptalene (**3**) which possesses the same ideal C_2 symmetry as the parent structure; however, it is much more twisted than the parent structure, and, in contrast to heptalene itself, it is conformationally and configurationally stable[13]). The electronic transitions in **3**, especially
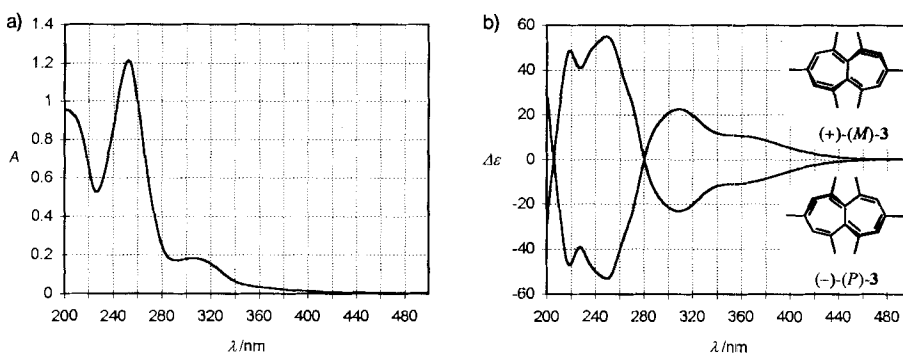

Fig. 6. *Spectra of 1,3,5,6,8,10-hexamethylheptalene* (**3**)[14]): a) *UV/VIS*, b) *CD* (hexane)

---

[13]) The real structure of heptalene is not known. It shows an extremely fast degenerate DBS process ($E_a < 3.5$ kcal mol^{-1} [40]), and the low-temperature ^{13}C-NMR spectrum of heptalene is in agreement with C_{2h} or C_2 symmetry of the skeleton. Dimethyl heptalene-3,8-dicarboxylate [43] may be taken as a border model for the parent structure. The X-ray crystallography of this diester [19] clearly reveals the non-planar C_2 symmetry of the heptalene skeleton with Θ (s-*cis*-butadiene) = -23.9 and $13.0°$ and Θ (s-*trans*-butadiene) = $140.8°$ of the perimeter, *i.e.*, the degree of twisting is much smaller than in other heptalenes (*cf. Scheme 3*). If we neglect the π- and σ-acceptor quality of the two MeOCO groups (see [44][45] for the effects of electron-donating and electron-withdrawing substituents on heptalenes), we may expect equal Θ (s-*cis*-butadiene) for heptalene itself in the order of the average of the diester, *i.e.*, of $18°$ (*cf.* **3** in *Scheme 3*).

[14]) This and all the following UV/VIS spectra of heptalenes have been measured with photodiode-array detector (wavelength accuracy: ± 1.5 nm) in hexane/4% i-PrOH.
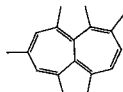
the long-wavelength transition can be seen much more clearly in the CD spectra of the antipodes of **3**. We see that there are at least two electronic transitions at wavelengths longer than 300 nm. The absorption band at 358 nm is very weak and broad, and nearly not recognizable in the UV/VIS spectrum. This band is followed, in the direction of shorter wavelengths, *i.e.*, higher transition energies, by a second more intense and broad, but well recognizable band at 310 nm. The third dominating absorption band appears at 250 nm and a further one shortly above 200 nm. The CD spectra of (+)-**3** and (−)-**3** indicate that **3** possesses further weak, however, optically active transitions at about 270 and 235 nm. The CD spectra of hexamethyl-heptalenes with a slightly different substitution pattern, like in the DBS isomers **9a** and **9b** (see *Table 2*), exhibit, as expected, quite similar UV/VIS and CD spectra. All heptalenes of this type, regardless of the substitution pattern, show a comparable electronic absorption behavior (*cf.* [25]) which is mainly governed by the degree of the twisting of the heptalene chromophor, *i.e.*, the smaller Θ (s-*cis*-butadiene) and the larger Θ (s-*trans*-butadiene), in a given series of heptalenes, is, the more pronounced will be the bathochromic shift of the discussed absorption bands, especially with respect to bands I and II. As an example, we may compare the position of I and II of the heptalene-4,5-dicarboxylate **15b** (*Scheme 4*) with its corresponding cyclic anhydride. In **15b**, the corresponding CD bands (cyclohexane) appear at 375 and *ca.* 350 nm (sh) of equal intensity [25]. The cyclic anhydride, however, exhibits the corresponding UV/VIS bands[15] at *ca.* 445 and 368 nm (hexane) [25]. The X-ray crystal structure of **15b** [11] shows Θ_{av}(s-*cis*-butadiene) = (33.2 ± 0.9)°, whereas the corresponding value for the cyclic anhydride of **15b** amounts to (27.1 ± 3.6)° [46].

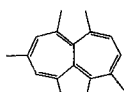Table 2. *CD Spectral Data of Hexamethylheptalenes*

Heptalene	Band positions [nm][a]					
	I	II	IIIa	IIIb	IIIc	IV
3[b]	358 (sh, 0.20)	310 (0.42)	269 (sh, 0.48)	249 (1.00)	238 (sh, 0.91)	219 (0.89)
9a[c]	350 (sh, 0.22)	310 (0.29)	260 (sh, 0.62)	248 (0.80)	240 (sh, 0.74)	217 (1.00)
9b[d]	347 (sh, 0.21)	313 (0.27)	–	249 (0.84)	240 (sh, 0.81)	217 (1.00)

[a]　In parentheses: relative intensities.

[b]　In hexane; data of both antipodes [16] (*cf. Fig. 6, b*).

[c] **9a**; in cyclohexane; data of the (−)-(*P*)-form [27].

[d] **9b**; in cyclohexane; data of the (−)-(*P*)-form [27].

[15]　Compare also the corresponding CD bands of the heptalene-4,5-dicarboxylate **1b** and its cyclic anhydride [25]. The spectral increment of the five-membered-ring anhydride with two C=O in planar arrangement with respect to the adjacent C=C bonds of the heptalene core amounts to *ca.* +20 nm when compared with the corresponding diester. The cyclic anhydride of diester **15b** racemizes too rapidly at room temperature for the measurement of its CD spectrum.

These general UV/VIS and CD properties are also displayed by benzo[a]heptalenes [47] as well as by heptaleno[1,2-c]furans [48]. The (−)-CE (CE = *Cotton* effect) for bands I and II, followed by a (+)-CE for band III is characteristic for the (P)-configuration at the central heptalene bond[16]).

Theoretical chemists have been interested in the structure of heptalene already over a long time (see *e.g.* lit. cited in [25] [50] [51]). Taking the monocyclic [12]annulene with its pairwise degenerated higher MO's in D_{12h} symmetry as starting point (*Scheme 13*), the symmetric introduction of the additional σ bond reduces the symmetry to D_{2h}. This planar delocalized heptalene possesses still one nonbonding molecular orbital. π-Bond localization reduces the symmetry further to C_{2h}, and most of the more advanced calculations were performed on this heptalene showing it to be more stable than D_{2h}-heptalene (*cf.* [51]). Twisting of the heptalene body in the sense of a C_2-loop leads finally to a non-planar C_2-heptalene, in agreement with all X-ray structures of heptalene derivatives, among which that of dimethyl heptalene-3,8-dicarboxylate [19] is probably at present still the closest to heptalene itself. In general terms, we may state that the C_2-heptalene will still have in its HOMOs and LUMOs some of the character of the two nonbonding MOs of its D_{12h}-great-grandfather, especially with respect to low-energy transitions between HOMOs and LUMOs, and the degree of twisting of the heptalene core must have a marked influence on these transitions as it has been found, indeed (*vide supra*).

Scheme 13

| D_{12h} | D_{2h} | C_{2h} | C_2 |
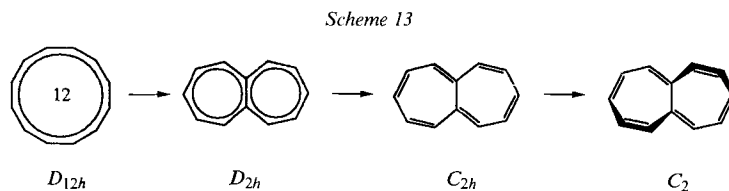
Buemi and *Zuccarello* [52] have performed extensive INDO/S-CI calculations with singly-excited electronic configurations as well as CNDO/S calculations with singly- plus doubly-excited electronic configurations of C_{2h}- and non-planar C_2-heptalene. The most relevant results are reproduced in *Table 3*. Without going too much into the details, one can see that both series of calculations lead to four distinguishable electronic transitions (*Entries 3–6*) which correspond quite well to the main absorption bands of **3** and its unsymmetrically substituted analogues **9a** and **9b** (*cf. Tables 2* and *3*). The tentative assignments become still more realistic, when we take into account that the longest-wavelength band of substituted heptalenes is very broad, reaching with its long-wavelength tail far beyond 400 nm (*cf. Fig. 6*). In *Sect. 3.2*, we will see that mainly the heptalene bands I and II are shifted and their intensities are modified by conjugating substituents on the heptalene core in both DBS isomers.

3.2. *Substituted Heptalene-1,2- and -4,5-dicarboxylate*s. All UV/VIS spectra which will be discussed here were measured directly in the HPLC apparatus with a photodiode-array detector, because a number of heptalene-dicarboxylates unterwent the thermal DBS

---

[16])   For MCD spectra of simply substituted heptalenes, see [49].

Table 3. *Calculated Most Relevant Electronic Transitions* ($\pi^* \leftarrow \pi$) *of* C_{2h}- *and* C_2-*Heptalene*[a])

Entry	INDO/S						
	Transition energy [eV]		Wavelength [nm]		Oscillator strength f		Symmetry for C_{2h}
	C_{2h}	C_2	C_{2h}	C_2	C_{2h}	C_2	
1	1.89	1.76	656	705	0	0	A_g
2	–	–	–	–	–	–	–
3	3.05	3.03	407	409	0.36	0.39	B_u
4	3.94	3.72	315	333	0.22	0.21	B_u
5	5.43	5.19	228	239	1.31	0.80	B_u
6	6.17	5.29	201	234	1.05	0.76	B_u

Entry	CNDO/S							
	Transition energy [eV]		Wavelength [nm]		Oscillator strength f		Symmetry for C_{2h}	Tentative assignment of **3**[b]) [nm]
	C_{2h}	C_2	C_{2h}	C_2	C_{2h}	C_2		
1	1.80	1.57	689	790	0	0	A_g	n.o.
2	3.26	3.30	380	376	0	0	A_g	n.o.
3	3.29	3.23	377	384	0.12	0.10	B_u	358 (sh, 0.20)
4	3.76	3.51	330	353	0.12	0.15	B_u	310 (0.42)
5	5.31	5.04	234	246	0.32	0.38	B_u	249 (1.00)
6	6.32	5.74	196	216	0.19	0.26	B_u	219 (0.89)

[a]) Only the lowest-energy and the most prominent transitions are given (for details, see [52]); the chosen non-planar form shows $\vartheta_{av} = (127 \pm 4)°$, *i.e.*, closely to ϑ_{av} of the heptalenes of this work (*cf. Table 1*).
[b]) Values taken from *Table 2*; n.o. = not observed.

process already at room temperature. However, in all cases we obtained well-resolved HPLC peaks for both DBS isomers. Only the DBS isomers, carrying merely three *peri*-substituents (*e.g.* **5a/5b** to **8a/8b**), showed already at room temperature a slight tendency of peak coalescence (*cf.* [53]). The HPLC conditions were the same for all heptalene-dicarboxylates (eluant: hexane/4% i-PrOH; flow rate: 1 ml/min; ambient temperature).

Figs. 7–9 (see also *Table 4*) demonstrate the influence of a systematic variation of the nature of a substituent at C(5) and C(1) on the habitus of the UV/VIS spectra of dimethyl 6,8,10-trimethylheptalene-1,2- and -4,5-dicarboxylates, respectively. The diesters **5a/5b** (*Fig. 7, a* and *b*) and **1a/1b** (*Fig. 7, c* and *d*), bearing no substituent or a Me group at C(5)/C(1), may be regarded as reference compounds. Their UV/VIS spectra are quite similar. However, two differences are remarkable. The less twisted diesters **5a** and **5b** show a much more pronounced tail of the extremely flat and broad band I as compared to the stronger twisted compounds **1a** and **1b**. Moreover, band I is moderately more intense and better separated from band II in **5a** and **1a**, where both MeOCO groups are in conjugation. This effect of conjugation is yet much clearer observed in the region of band III. Whereas **5b** and **1b** exhibit here a comparably flat and broad, nonstructured absorption, the DBS isomers **5a** and **1a** are marked by an intense absorption at 269 nm. No doubt, this is a first indication that the 1,2-CS set-up of the A-type (*cf. Scheme 2*) is in action.

Table 4. *UV/VIS Spectra of Dimethyl 6,8,10-Trimethylheptalene-1,2- and -4,5-dicarboxylates Carrying Substituents at C(5) and C(1), Respectively*

Heptalene		λ_{max} [nm][b]				Fig.
No.	Code[a]	I	II	III	IV	
5a	–	*ca.* 400 (0.04)	318 (sh, 0.19)	269 (1.00)	238 (sh, 0.71)	*7, a*
5b		*ca.* 400 (0.03)	328 (sh, 0.25)	280 (sh, 0.88)	261 (1.00)	*7, b*
1a	[Me5]	390 (0.03)	318 (sh, 0.13)	268 (1.00)	233 (sh, 0.81)	*7, c*
		[388 (0.31)][c]	[318 (0.30)]	[280 (1.00)]	[227 (0.50)]	
				[272 (sh, 0.86)]		
1b	[Me1]	*ca.* 370 (sh, 0.06)	320 (sh, 0.17)	*ca.* 280 (sh, 0.87)	261 (1.00)	*7, d*
					236 (sh, 1.00)	
		[369 (0.56)]	[327 (0.57)]	[280 (1.00)]	[251 (0.88)]	
11a	[St5]	*ca.* 400 (sh, 0.02)	345 (sh, 0.37)	285 (1.00)	235 (sh, 0.73)	*8, a*
		[400 (sh, 0.10)]	[350 (0.17)]	[285 (1.00)]	[239 (sh, 0.13)]	*8, c*
					[234 (0.13)]	
11b	[St1]	*ca.* 400 (sh, 0.22)	355 (sh, 0.55)	321 (1.00)	262 (0.61)	*8, b*
					ca. 220 (sh, 0.74)	
		[403 (0.84)]		[306 (1.00)]	[252 (0.49)]	*8, d*
					[220 (0.45)]	
12a	[ClSt5]	*ca.* 400 (sh, 0.02)	345 (sh, 0.41)	287 (1.00)	240 (0.58)	*7, e*
12b	[ClSt1]	*ca.* 400 (sh, 0.23)	355 (sh, 0.61)	323 (1.00)	262 (0.61)	*7, f*
					220 (sh, 0.74)	
13a	[MeOSt5]	*ca.* 400 (sh, 0.02)	328 (sh, 0.72)	293 (1.00)	240 (sh, 0.67)	*8, e*
13b	[MeOSt1]	*ca.* 400 (sh, 0.48)	360 (sh, 0.79)	330 (1.00)	265 (0.70)	*8, f*
					228 (sh, 0.84)	
10a	[MeOPh5]	395 (0.03)	*ca.* 320 (sh, 0.18)	284 (sh, 0.79)	240 (1.00)	*9, a*
				267 (sh, 0.86)		
10b	[MeOPh1]	*ca.* 390 (sh, 0.19)	*ca.* 340 (0.45)	311 (0.87)	225 (1.00)	*9, b*
				283 (sh, 0.75)		

[a]   Nature and position of the additional substituent: St = (*E*)-styryl; ClSt = (*E*)-4-chlorostyryl; MeOSt = (*E*)-4-methoxystyryl; MeOPh = 4-methoxyphenyl.

[b]   In parentheses are the relative intensities of the absorption bands.

[c]   In brackets are the corresponding extrema of the CD spectra in hexane or cyclohexane; values for **1a** and **1b**: see [1a] [25].

Nevertheless, the spectral habitus undergoes much more changes, when the 1,4-CS system is activated by the introduction of an (*E*)-styryl substituent at C(5)/C(1) (*Fig. 8, a* and *b*). Heptalene **11a** shows now in the band-II region an intense and, at the higher-frequency side, faintly asymmetric absorption band at 285 nm. The bathochromic wavelength shift of at most 16 nm as compared to **1a** can be attributed to the presence of the conjugative (*E*)-styryl group at C(5). The effect of conjugation is more dramatically seen at band II. This band appears as a just visible shoulder in **1a**, but is well expressed in the corresponding CD spectra with the extrema at 318 nm (*cf. Table 4*). On the other hand, a distinct hyperchromic effect and bathochromic shift of this band is recognizable in **11a**. It is situated at 345 nm as a strong, well-visible shoulder. Again, the CD spectra of **11a** (*Fig. 8, c*)[17]) give the clearer answer in showing the extrema of the corresponding CD

[17])   The CD spectra of (+)-(*M*)- and (−)-(*P*)-**11a** show the typical habitus of C_2-heptalenes with the characteristic sequence (+)/(+)/(−) and *vice versa* of the CEs (*cf.* [25]). The antipodes of **11a** were separated by HPLC on an analytical *Chiralcel* column. Thermal rearrangement of (+)-(*M*)- and (−)-(*P*)-**11a** at 80° gave quantitatively (+)-(*M*)- and (−)-(*P*)-**11b** (for details, see *Exper. Part*).
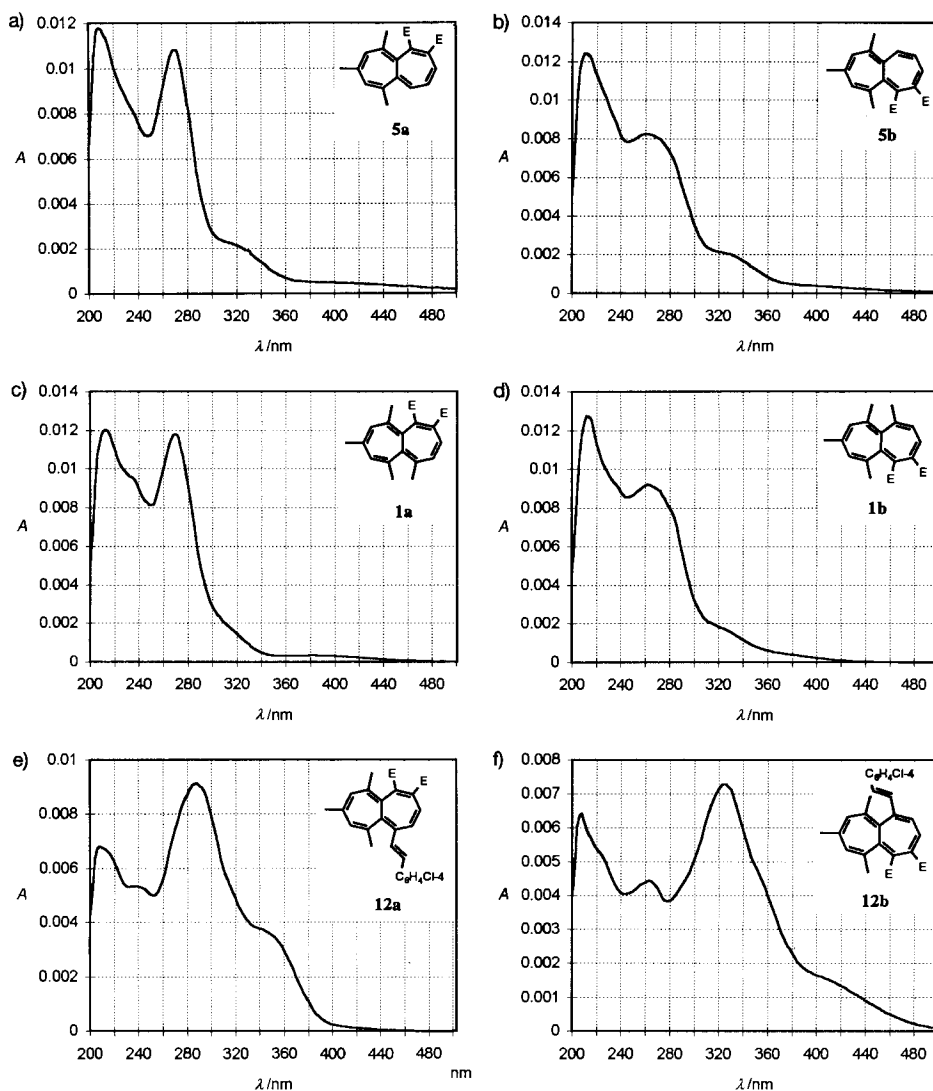
Fig. 7. *UV/VIS Spectra of* a) **5a**, b) **5b**, c) **1a**, d) **1b**, e) **12a**, f) **12b**

bands at 350 nm (*Table 4*). The region of band I is almost not altered in going from **1a** to **11a**. In both cases, we find a weak broad absorption band around 400 nm. When the 1,4-CS system is turned on photochemically, we observe a substantial change in the UV/VIS behavior of **11b**. Band III is shifted from 285 nm (**11a**) to 321 nm, leading to the phenomenon that band II at 355 nm is nearly buried under the long-wavelength flank of this band (*cf. Fig. 8, b*). Most important, however, is the effect of the 'through-conjugation' between the (*E*)-styryl substituent at C(1) and the MeOCO group at C(4) on band I. It is strongly enhanced but only slightly shifted in its maximum. Still more dramatic are
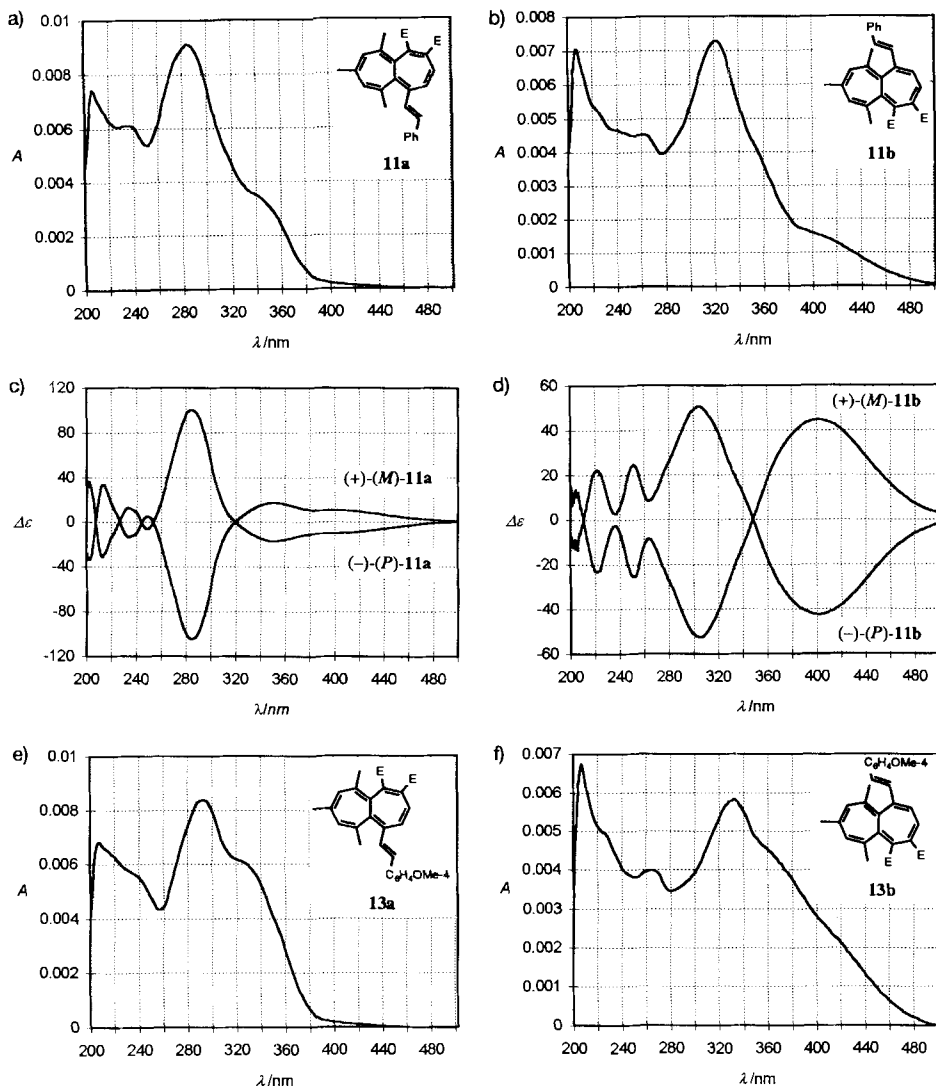
Fig. 8. *UV/VIS Spectra of* a) **11a**, b) **11b**, e) **13a**, f) **13b**, *and CD spectra of* c) (+)-(M)- *and* (–)-(P)-**11a**,
d) (+)-(M)- *and* (–)-(P)-**11b**

the effects on the CD spectra of **11b** (*Fig. 8, d*)[17]). The CD spectrum, *e.g.* of (–)-(*P*)-**11a**, is still heptalene-like (*cf.* [25]). The on-state of the 1,4-CS system in (–)-(*P*)-**11b**, however, generates a superposition of the (–)-CEs of band I and II to a single immense band with its maximum at 403 nm and its long-wavelength tail at above 500 nm. The (+)-CE at 306 nm corresponds with band III in the UV/VIS spectrum.

There is nearly no change in the UV/VIS spectra, when we compare that of **11a** and **11b** with those of the *p*-Cl derivatives **12a** and **12b** (*cf. Fig. 7, e* and *f*, and *Table 4*). Again
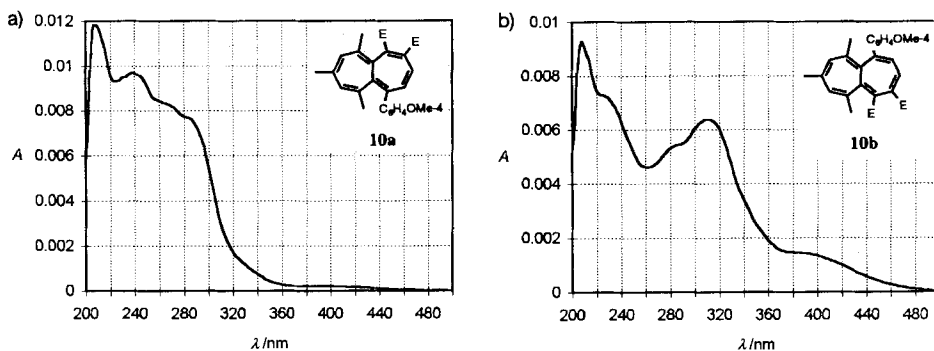
Fig. 9. *UV/VIS Spectra of* a) **10a**, b) **10b**

is band II in the on-state (*Fig. 7,f*) almost not recognizable, because it is nearly covered by the long-wavelength flank of the massive band III at 323 nm. The situation is still much more accentuated in the UV/VIS spectra of the heptalenes **13a** and **13b** (*cf. Fig. 8,e* and *f*, and *Table 4*) with the MeO group as strong π-donor substituent in *para*-position of the (*E*)-styryl moiety. In the off-state (*Fig. 8*), the longest-wavelength band at *ca.* 400 nm is only very weakly visible, whereas band II at 328 nm appears as an enormous shoulder on the long-wavelength flank of band III, now at 293 nm. The photochemically activated on-state (*Fig. 8,f*) is characterized by a nearly steady increase of absorption from 500 to 330 nm the λ_{max} point of the dominating band III. Band I and II can merely weakly be recognized at *ca.* 400 and 360 nm. If we compare the relative absorption intensities at 400 nm (band I), we find a *ca.* 25-fold absorption difference between the off- and the on-state. The UV/VIS spectra of the 4-methoxyphenyl-substituted heptalenes **10a** and **10b** (*cf. Fig. 9,a* and *b*, and *Table 4*) reveal that the π-donor effect of the MeO group is in these cases not as well transmitted to the heptalene π-core as in the cases of **13a** and **13b**.

The effect of 'through-conjugation' in the on-state of the 6,8,10-trimethyl-substituted heptalene-dicarboxylates, all representing heptalenes with four *peri*-substituents and, thus, with highly twisted π perimeters, is also found in the heptalenes derived from corresponding guaiazulenes. These heptalene-dicarboxylates with three *peri*-substituents are permanently in the on-state, what means that the off-state is thermodynamically and kinetically too unstable to be visible at room temperature. We see that the reference compounds **14b** and **15b** show UV/VIS spectra (*Fig. 10,a* and *b*; see also *Table 5*) which are almost identical with those of the analogues **5b** and **1b** (*cf. Fig. 7,b* and *d*) in the former series. Also the introduction of an (*E*)-styryl substituent at C(1) creates a habitus of the UV/VIS spectrum of **16b** (*cf. Fig. 10,c*, and *Table 5*) which is fully comparable with that of **11b** (*Fig. 8,b*). The attachment of a MeO substituent at the *para*-position of the (*E*)-styryl group demonstrates again the strong donor-acceptor conjugation in **17b** (*Fig. 10,d*, and *Table 5*). However, since the ring system of **17b** is slightly flatter, *i.e.*, less twisted than that of **11b**, we observe more pronounced bathochromic shifts of band I and II as compared to **11b**. As a result, the two shoulders of band I and II, respectively, placed on the flank of band III, are better visible than in the spectrum of **11b**.

Table 5. *UV/VIS Spectra of Dimethyl 9-Isopropyl-6(or 1)-methylheptalene-4,5-dicarboxylates Carrying Substituents at C(1) or C(6)*

Heptalene		λ_{max} [nm][b]				Fig.
No.	Code[a]	I	II	III	IV	
14b	–	ca. 400 (sh, 0.03)	ca. 340 (sh, 0.20)	ca. 272 (sh, 0.91)	247 (1.00)	10,a
15b	[Me1]	ca. 390 (sh, 0.04)	ca. 335 (sh, 0.17)	280 (sh, 0.83)	250 (1.00)	10,b
		[375 (0.40)][c]	[350 (sh, 0.35)]	[277 (1.00)]	[255 (sh, 0.72)]	
16b	[St1]	400 (sh, 0.22)	ca. 360 (sh, 0.45)	320 (1.00)	260 (0.60)	10,c
17b	[MeOSt1]	ca. 420 (sh, 0.36)	ca. 360 (sh, 0.68)	330 (1.00)	260 (0.63)	10,d
18b	[St6]	ca. 400 (sh, 0.17)	ca. 350 (sh, 0.39)	311 (sh, 0.94)	259 (0.93)	10,e
				304 (1.00)	240 (sh, 0.87)	
19b	[MeOSt6]	ca. 400 (sh, 0.22)	ca. 350 (sh, 0.51)	314 (1.00)	259 (0.88)	10,f
					240 (sh, 0.83)	

[a]) See *Footnote a* in *Table 4*.   [b]) In parentheses are the relative intensities of the absorption bands.   [c]) In brackets are the corresponding extrema of the CD spectrum of **15b** in cyclohexane [25].
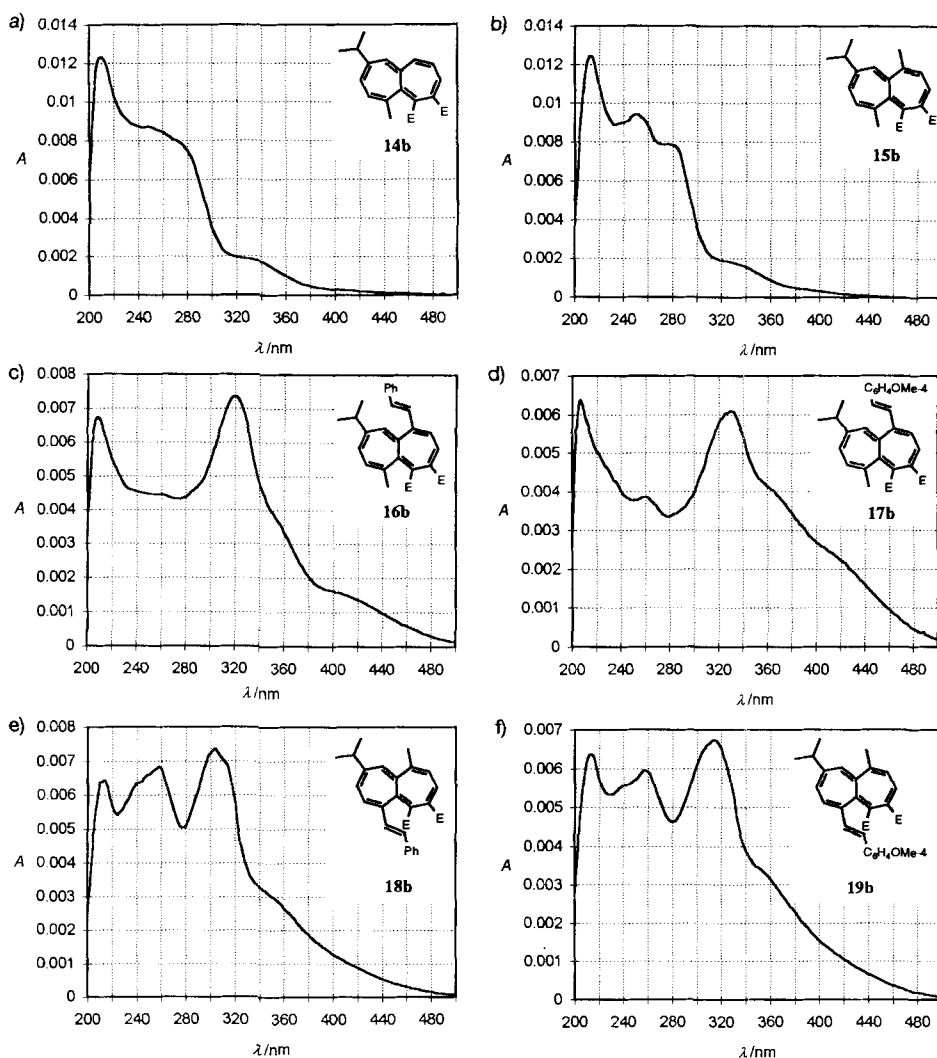
Fig. 10. *UV/VIS Spectra of* a) **14b**, b) **15b**, c) **16b**, d) **17b**, e) **18b**, f) **19b**

In this series of guaiazulene-derived heptalene-4,5-dicarboxylates, we also synthesized pendants to **16b** and **17b**, namely the heptalenes **18b** and **19b**, which are structurally characterized by an exchange of the substituents at C(1) and C(6) as compared to **16b** and **17b**. A comparison of the UV/VIS spectra of **18b** (*Fig. 10,e*) and of **16b** (*Fig. 10,c*) manifests that there is a great similarity in the long-wavelength region. Band I of **18b** is not clearly recognizable, and band II appears as a weakly developed shoulder at *ca.* 350 nm. Band III of **18b** is slightly splitted with the main absorption at 304 nm. In comparison to the spectrum of **16b**, it is quite obvious that the acceptor-donor set-up in **16b** creates the more intense band I and II, when band III is taken as reference. These effects are much more pronounced when we compare the π-donor-substituted pair **17b** and **19b** (*Fig. 10,d* and *f*). Whereas there is a great change in the UV/VIS spectra when we go from **16b** to **17b**, both with the π-acceptor group (MeOCO) in 'through-conjugation', only slight changes are recognizable when we move from **17b** to **19b**, due to the fact that both compounds carry the i-Pr group in 'through-conjugation' instead of a π-acceptor group.

In the last set of heptalenes (*cf. Table 6* and *Fig. 11*), we studied the effect of 'through-conjugation' with the MeOCO group at C(1) and C(5), respectively, in correspondingly substituted 6,8,10-trimethylheptalene-1,2- and -4,5-dicarboxylates. The reference compounds are the heptalene-dicarboxylates **6a** and **6b** carrying again only a Me group at C(4) and C(2), respectively. As expected, their UV/VIS spectra (*Fig. 11,a* and *b*) resemble closely those of **1a** and **1b** (*Fig. 7,c* and *d*), or **5a** and **5b** (*Fig. 7,a* and *b*). However, the habitus of the spectra is changed, when the Me group is replaced by the (*E*)-styryl moiety. Compound **8a** (*Fig. 11,c*), representing now the on-state of the 1,4-CS set-up, shows an enhanced band I at *ca.* 400 nm, and band II is completely buried under the massive flank of band III at 320 nm. The additional band appearing at 285 nm indicates the co-existence of the on-state of the 1,2-CS system of the two ester groups. The thermal switch to **8b** (*Fig. 11,d*) turns off both conjugations. The long-wavelength flank of band III is in this state much steeper or, in other words, there must be a tremendous decrease in the relative intensity of band II, still buried under the tail of band III. The whole habitus of the long-wavelength region of **8b** also discloses a weaker intensity of band I, which is only indicated by the recognizable long tailing. The situation in the Ph-substituted heptalenes **7a** and **7b** (*Fig. 11,e* and *f*) is quite similar to that of **6a** and **6b**. However, the absorption bands in the UV/VIS spectra are a bit less structured (see also *Table 6*). The 'through-conjugation' in **7a** is clearly recognizable by the impressive flank at the long-wavelength end of band III, which hides band II and resembles in its upper part that of **6a**, *i.e.*, it indicates also the 'through-conjugation' of the two ester groups in **7a**. The broad absorption of band I at 400 nm is more intense than in **6a**. The habitus of the spectra of **7b** and **6b** are very close to each other, in agreement with the fact that both compounds are in the double off-state.

A last point should be discussed, namely the question whether the observed effects of the π substituents on the position and the intensities[18]) of the heptalene bands I–III are in agreement with the calculated character of these electronic transitions. According to *Buemi* and *Zuccarello*'s INDO/S calculations, the excited electronic states of C_{2h}-hep-

---

[18]) We consider here intensities as absorption coefficients at a given λ_{max} value and not as the reliable integrated band intensities.

Table 6. *UV/VIS Spectra of Dimethyl 6,8,10-Trimethylheptalene-1,2- and-4,5-dicarboxylates Carrying Substituents at C(4) and C(2), Respectively*

Heptalene		λ_{max} [nm][b]				Fig.
No.	Code[a]	I	II	III	IV	
6a	[Me4]	*ca.* 390 (sh, 0.03)	320 (sh, 0.19)	269 (1.00)	235 (sh, 0.73)	–
6b	[Me2]	*ca.* 400 (sh, 0.03)	325 (sh, 0.25)	284 (0.87)	259 (1.00)	–
8a	[St4]	410 (sh, 0.09)	320 (1.00)	285 (0.88)	224 (sh, 0.72)	–
8b	[St2]	*ca.* 400 (sh, 0.07)	314 (1.00)	287 (sh, 0.78)	–	–
7a	[Ph4]	400 (0.04)	n.o. *ca.* 300 (sh, 0.69)	276 (1.00)	250 (0.73) 220 (sh, 0.95)	–
7b	[Ph2]	*ca.* 400 (sh, 0.03)	340 (sh, 0.21)	294 (sh, 0.68) 263 (0.83)	237 (0.97) 227 (0.74)	–

[a]) See *Footnote a* in *Table 4*.　[b]) In parentheses are the relative intensities of the absorption bands.
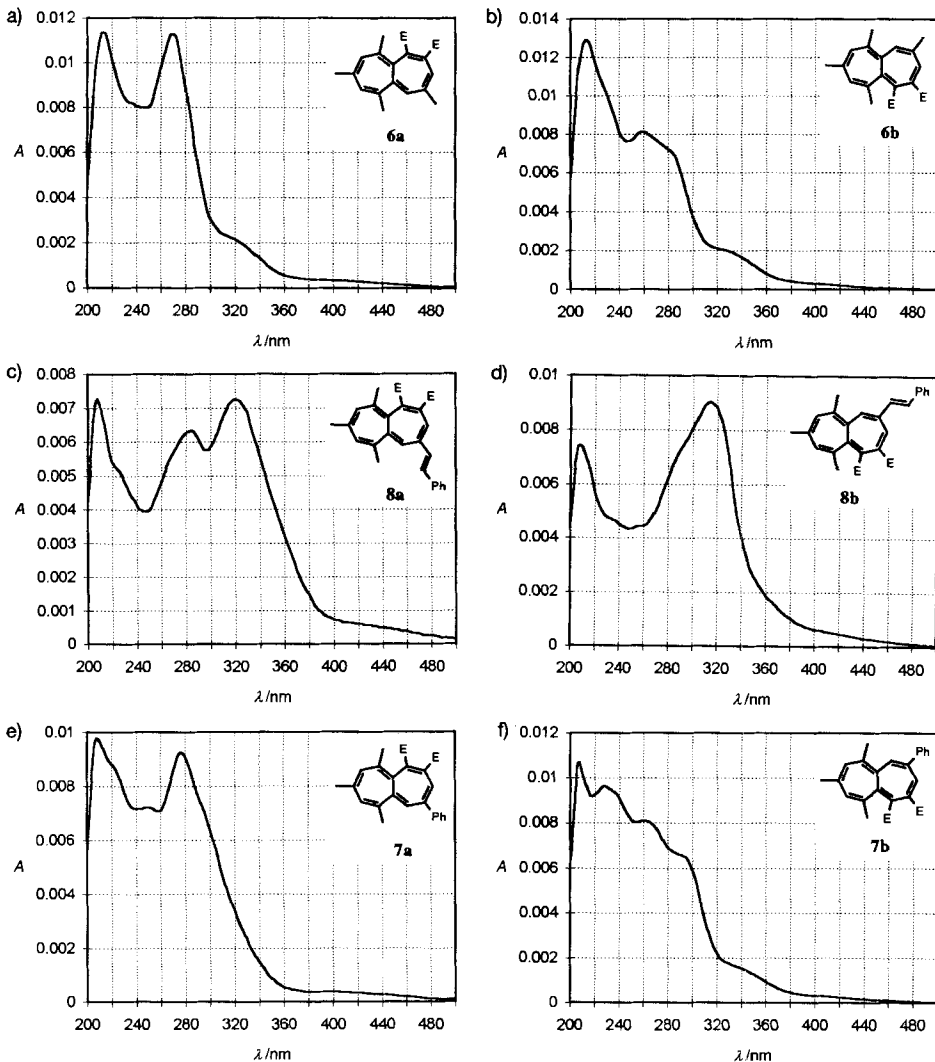
Fig. 11. *UV/VIS Spectra of* a) **6a**, b) **6b**, c) **8a**, d) **8b**, e) **7a**, f) **7b**

talene (*cf. Table 3*) [52] give rise to band I which consists to 88% of the HOMO→NLUMO transition, to band II which consists to 81% of the HOMO→NNLUMO (*cf. Fig. 12*) and to 10% of the NHOMO→LUMO transitions, and finally to band III which consists to 79% of the NHOMO→LUMO transition. These electronic transitions can be characterized by their transition densities (see [54] and the discussion therein). As there is a clear correlation of the nodal properties of the MOs of heptalene calculated with assumed D_{2h}, C_{2h}, and C_2 geometry, the MO set of the D_{2h}-heptalene (*cf. Fig. 12*) can be used for a qualitative discussion of the variously twisted C_2-heptalenes[19]).
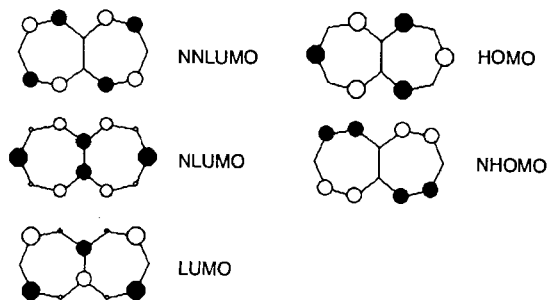

Fig. 12. *Upper occupied and lower unoccupied molecular orbitals of* D_{2h}*-heptalene*

Transition densities can be approximated by transition monopoles which, in turn, are the product of the MO coefficients, on the same atom, of the orbitals involved in the electronic transition. This provides an easy way to visualize the polarization of the electronic transitions. An inspection of *Fig. 12* immediately reveals that the visible longest-wavelength transition of heptalene (band I) should be polarized along the heptalene axis which passes through C(3) and C(8) and cuts the central σ bond. On the other hand, the next transition (band II) should be polarized perpendicularly to the heptalene axis, *i.e.*, the polarization is in the direction of the central σ bond. The third transition (band III) should be polarized again along the heptalene axis. These predictions are in reasonable, but not perfect agreement with the experimental facts. They tell us that, in all optically active heptalenes so far investigated, band I and II show always the same sign of their CEs, followed always by sign inversion for the CE of band III (*cf., e.g., Fig. 6, b* and *Fig. 8, c* and *d*). The (*P*)-configuration of the heptalenes is thereby characterized by two (−)-CEs of band I and II, followed by an intense (+)-CE for band III, and *vice versa* for the (*M*)-configurated heptalenes (see also [25]). (*P*) and (*M*) describe thereby the sense of chirality of the torsion at the central σ bond. The topology of C_2-heptalene is identical with that of a C_2-loop. It is a general property of C_2-loops that their topological chirality is opposite along their two molecular axes (not the C_2-axis). That this is true for heptalenes has experimentally been demonstrated by *Gottarelli, Hansen*, and coworkers [55]. Simply according to the polarization of the electronic transitions of the D_{2h}-heptalene, one would

---

[19]) A more detailed discussion on the UV/VIS and CD spectra of heptalenes, especially those of **3** (*cf. Fig. 6, a* and *b*), will follow in this journal.

predict the sign pattern $(\pm)/(\mp)/(\pm)$ for the CEs of band I, II, and III of C_2-heptalene. The change of sign predicted between band II and III is hence correct. According to this reasoning, band I shows the wrong sign. Yet, the calculations of *Buemi* and *Zuccarello* show that already in C_{2h}-heptalene the orbital coefficients at C(3) and C(8) in the HOMO become much smaller than in D_{2h}-heptalene and grow at the other C-atoms, and especially at C(1) and C(6). The NLUMO of D_{2h}-heptalene possesses large orbital coefficients at C(1), C(3), C(6), and C(8). As a consequence, the transition densities of the longest-wavelength transition are mostly found on C(1) and C(6). This means, however, that the vector of polarization is turned towards the direction of the axis of the central σ bond. This may explain the experimental results that the longest-wavelength transition of optically active heptalene shows always the same sign of the CE as band I (see also [25]).

The above observations lend support to the assignment proposed for the electronic transitions of heptalenes (*cf. Table 3*). A further support comes from the effects observed for conjugative substituents at C(5) on the intensity of band II as is evident from a comparison of the UV/VIS spectra of **1a**, **11a**, **12a**, and **13a** (*Fig. 7,c, Fig. 8,a, Fig. 7,e,* and *Fig. 8,e*)[19]). There is a clear increase of the intensity of this band with an increase of the π-donor quality of the substituent at C(5). This observation is in agreement with the polarization predicted in the direction mainly along the central σ bond for this electronic transition.

In the meantime, we learned how to modify chemically heptalene-4,5-dicarboxylates. This allowed us to attach much more extended π-systems to the heptalene core [56]. As a first result, methyl 9-isopropyl-6-methyl-1,4-bis(4-phenylbuta-1,3-dien-1-yl)heptalene-5-carboxylate, the on-state structure, possesses a strong absorption band at 433 nm which disappears in the corresponding DBS isomer, representing the off-state structure (*cf.* [57]).

Experimental Part

General. See [24] and lit. cited there. HPLC: on a *Waters 911* instrument with photodiode array detector (optical resolution: ± 1.5 nm) with the following columns: *Spherisorb CN* (ODS 5 μm; length 250, diam. 4.6 mm) for anal. runs, and *Chiralcel OD* (length 250, diam. 4.6 mm) from *Daicel Chemical Industries*, equipped with a corresponding pre-column (length 50 mm, diam. 4.6 mm), for optical resolutions. Mobile phase for the UV/VIS spectra: hexane/4% i-PrOH (flow rate: 1 ml/min). CD Spectra: on a *Jasco* spectropolarimeter (model *J-500A*).

Dimethyl Heptalene-dicarboxylates. – 1. *6,8,10-Trimethyl-4-[(E)-2-phenylethenyl]heptalene-1,2-dicarboxylate and 6,8,10-Trimethyl-2-[(E)-2-phenylethenyl]heptalene-4,5-dicarboxylate* (**8a** and **8b**, resp.). Both DBS isomers form at r.t. a thermal equilibrium mixture consisting of 25% of **8a** and 75% of **8b** [24]. ^{1}H-NMR of **8a** (600 MHz, CDCl$_3$; taken from the 1:3 mixture **8a**/**8b**[20])): 7.42 ($d, J = 7.6$, 2 H$_o$ of Ph); 7.32 ($t, J = 7.5$, 2 H$_m$ of Ph);

7.25 (t, partly covered by CHCl$_3$, H$_p$ of Ph); 6.80 (AB, $\Delta\delta$ < 1, $J_{AB} \approx$ 16.6. PhCH=CH); 6.57 (s, H–C(3)); 6.15 (s, H–C(5)); 6.11 (s, H–C(9)); 5.96 (s, H–C(7)); 3.85, 3.73 (2s, 2 MeOCO); 2.19 (s, Me–C(6)); 2.00 (s, Me–C(8)); 1.67 (s, Me–C(10)). ^{1}H-NMR of **8a** (300 MHz, C$_6$D$_6$; taken from the 1:3 mixture **8a/8b**[20])[21]): 6.84 (s, H–C(3)); 6.64, 6.61 (AB, $\Delta\delta$ = 9.8, J_{AB} = 16.3, PhCH=CH with PhCH= at 6.64); 6.21 (s, H–C(5)); 6.00 (s, H–C(9)); 5.77 (s, H–C(7)); 3.56, 3.40 (2s, 2 MeOCO); 2.07 (br. s, Me–C(8)); 1.74 (br. s, Me–C(6)); 1.73 (s, Me–C(10)). ^{1}H-NOE (600 MHz, C$_6$D$_6$): 6.64 (PhCH=CH)→7.05 (m, 2 H$_o$ of Ph), 6.84 (m, H–C(3)); 6.21 (s, H–C(5)); 6.61 (PhCH=CH)→7.05 (s, 2 H$_o$ of Ph), 6.84 (s, H–C(3)), 6.21 (m, H–C(5)). The results show that the s-*trans*-conformation is preferred around the C(4)–C(1′) bond in the structural segment C(3)=C(4)–C(1′)=C(2′). ^{1}H-NMR of **8b** (600 MHz, CDCl$_3$, taken from the 1:3 mixture **8a/8b**): 7.93 (s, H–C(3)); 7.47 (d, J = 7.6, 2 H$_o$ of Ph); 7.35 (t, J = 7.8, 2 H$_m$ of Ph); 7.26 (t, H$_p$ of Ph); 6.93, 6.77 (AB, J_{AB} = 16.3, PhCH=CH with PhCH= at 6.93); 6.16 (s, H–C(9)); 6.15 (s, H–C(1)); 5.96 (s, H–C(7)); 3.77, 3.70 (2s, 2 MeOCO); 2.04 (br. s, Me–C(8)); 2.00 (s, Me–C(6)); 1.81 (s, Me–C(10)). ^{1}H-NMR of **8b** (300 MHz, C$_6$D$_6$; taken from the 1:3 mixture **8a/8b**): 8.27 (s, H–C(3)); 6.77 (AB, $\Delta\delta$ = < 1, $J_{AB} \approx$ 16.8, PhCH=CH); 6.07 (s, H–C(1)); 6.02 (s, H–C(9)); 5.89 (s, H–C(7)); 3.45, 3.29 (2s, 2 MeOCO); 2.08 (br. s, Me–C(8)); 2.08 (br. s, Me–C(6)); 1.68 (s, Me–C(10)). ^{1}H-NOE (600 MHz, CDCl$_3$): 6.93 (PhCH=CH)→7.47 (m, 2 H$_o$ of Ph), 6.77 (s, PhCH=CH), 6.15 (s, H–C(1)); 6.77 (PhCH=CH)→7.93 (s, H–C(3)), 7.48 (s, 2 H$_o$ of Ph), 6.93 (s, PhCH=CH). The results show that the s-*trans*-conformation is preferred around the C(2)–C(1′) bond in the structural segment C(1)=C(2)–C(1′)=C(2′). UV of **8a** see *Table 6* and *Fig. 11,c*; UV of **8b**: see *Table 6* and *Fig. 11,d*.

The structure of **8b** was also determined by an X-ray crystal-diffraction analysis (see *Tables 1* and *7* as well as *Fig. 1*).

1.1. *6,8,10-Trimethyl-4-{(E)-2-phenyl[1-^{2}H]ethenyl}heptalene-1,2-dicarboxylate and 6,8,10-Trimethyl-2-{(E)-2-phenyl[1-^{2}H]ethenyl}heptalene-4,5-dicarboxylate* ([1′-^{2}H]-**8a** and [1′-^{2}H]-**8b**, resp.). Methyl 4,6,8-tri-methylazulene-2-carboxylate [30] was reduced with LiAl[^{2}H$_4$] and subsequently reacted with MnO$_2$ in CH$_2$Cl$_2$ at r.t. to yield 4,6,8-trimethylazulene-2-[^{2}H]carbaldehyde with a [^{2}H]-content of > 99% (*cf.* [31]). Reaction of this [^{2}H]carbaldehyde with benzytriphenylphosphonium chloride in EtOH in the presence of EtONa gave, after thermal $(Z)/(E)$-isomerization with I$_2$ in toluene (80°/50 min), pure 4,6,8-trimethyl-2-[(E)-2-phenyl-[1-^{2}H]ethenyl]azulene in 84% yield (*cf.* [24]). Thermal reaction of this azulene (0.0588 g; 0.215 mmol) with dimethyl acetylenedicarboxylate (0.069 g; 0.48 mmol) in decalin (1 ml) at 190°/2 h led to the formation of [1′-^{2}H]-**8a**/[1′-^{2}H]-**8b** (0.0255 g, 29%) and of *dimethyl trans-6-[(Z)-1,2-bis(methoxycarbonyl)ethenyl]-10,12,14-trimethyl-5-phenyl[6-^{2}H]tricyclo[7.5.0.0^{2,7}]tetradeca-1(14),2(7),3,8,10,12-hexaene-3,4-dicarboxylate* (0.0215 g, 18%). The ^{1}H-NMR (300 MHz, CDCl$_3$) of the latter compound showed only a s for 1 H at 4.34, indicating that no H at C(6) was present (*cf.* [24]). ^{1}H-NMR (300 MHz, CDCl$_3$ as well as C$_6$D$_6$) of the 1:3 mixture [1′,^{2}H]-**8a**/[1′-^{2}H]-**8b** showed PhCH= of [1′-^{2}H]-**8a** (C$_6$D$_6$) as s at 6.64 and of [1′-^{2}H]-**8b** (CDCl$_3$) as s at 6.76. ^{1}H-NOE (400 MHz, CDCl$_3$) of [1′-^{2}H]-**8a** in the 1:3 mixture: 6.80 (PhCH=C[^{2}H])→7.42 (m, 2 H$_o$ of Ph), 6.57 (w, H–C(3)), 6.15 (s, H–C(5)); integration of the signal at 6.57 and 6.15 gave a ratio of 1:7.3; 6.57 (H–C(3))→6.80 (w, PhCH=C[^{2}H]). ^{1}H-NOE of [1′-^{2}H]-**8b**: 6.76 (PhCH=C[^{2}H])→7.93 (s, H–C(3)), 7.47 (m, 2 H$_o$ of Ph), 6.15 (vw, H–C(1)[22]); integration of the signals at 7.93 and 6.15 gave a ratio of 12:1 which has to be regarded as the lower limit; 6.15 (H–C(1))→no recognizable effect at 6.76 (PhCH=C[^{2}H]).

2. *6,8,10-Trimethyl-4-phenylheptalene-1,2-dicarboxylate and 6,8,10-Trimethyl-2-phenylheptalene-4,5-dicar-boxylate* (**7a** and **7b**, resp.). 4,6,8-Trimethyl-2-phenylazulene (0.292 g, 1.00 mmol) [35] and dimethyl acetylenedicar-boxylate (0.215 g; 1.50 mmol) were heated in decalin (4 ml) for 5 h at 190°. Further dimethyl acetylenedicarboxylate (0.215 g; 1.50 mmol) was added and heating continued for additional 3 h, until more of the azulene was consumed (TLC control). All volatile material was removed at 50°/high vacuum and the residue chromatographed on silica gel with hexane/Et$_2$O (7:3). Four fractions were obtained. The first one contained non-consumed azulene (0.030 g,

---

[20]) For the sake of clarity, we report here again the ^{1}H-NMR spectrum of **8a** and **8b** in CDCl$_3$ (*cf.* [24]), because we changed the locants of the heptalene skeleton according to the new IUPAC recommendations (*cf.* [7]). Moreover, according to ^{1}H-NOE mesurements, we had to exchange the chemical shifts of H–C(5) (H–C(1) in [24]) and H–C(9) (H–C(7) in [24]) as well as of Me–C(6) (Me–C(10) in [24]) and Me–C(8) (also Me–C(8) in [24]) in **8a**.

[21]) The signals of the Ph group are partly covered by the solvent signal (C$_6$D$_5$H).

[22]) We cannot completely exclude that a part of this signal belongs to that of H–C(5) of [1′-^{2}H]-**8a** due to partial irradiation of PhCH=C[^{2}H] of [1′-^{2}H]-**8a** at 6.80 ppm. However, in this case one would also expect a weak effect on 2 H$_o$ of Ph at 7.42 ppm of this DBS isomer. This was not observed.

10%), the second one dimethyl *(E)-1-(4,6,8-trimethyl-2-phenylazulen-1-yl)ethene-1,2-dicarboxylate* ((*E*)-**20**; 0.015 g; 4%), the third one a 23:77 mixture **7a/7b** (0.140 g; 36%), and the last one dimethyl 4,6,8-trimethylazulene-1,2-dicarboxylate (0.034 g; 12%) [25].

Data of (E)- **20**. Brown needles. M.p. 147.5–148.5° (Et$_2$O/hexane). UV (MeOH): λ_{max} 397 (4.19), 305 (4.95), 248 (4.65). IR (CHCl$_3$): 3030*w*, 2930*m*, 2860*m*, 1720*s*, 1600*m*, 1430*m*, 1260*s*, 1020*m*, 820*m*. ^{1}H-NMR (300 MHz, CDCl$_3$): 7.36 (*m*, 5 arom. H, H–C(3)); 7.08 (*s*, MeOCOC*H*=); 7.03 (*s*, H–C(5,7)); 3.74, 3.36 (2*s*, 2 MeOCO); 2.88 (*s*, Me–C(4)); 2.76 (*s*, Me–C(8)); 2.60 (*s*, Me–C(6)). CI-MS: 391 (7), 390 (23), 389 (100, [*M* + 1]$^+$). EI-MS: 389 (23), 388 (100, *M*$^{+}$), 330 (21), 329 (98, [*M* – COOMe]$^+$), 328 (26), 298 (50), 297 (50, [*M* – COOMe – MeOH]$^+$), 271 (9), 270 (43, [*M* – 2 COOMe]$^+$), 269 (32).

Data of **7a**. Thermal equilibrium amount at r.t. in the presence of **7b** is 23%. UV: See *Table 6* and *Fig. 11,a*. ^{1}H-NMR (300 MHz, CDCl$_3$; in the presence of 77% of **7b**): 7.51–7.31 (*m*, 5 arom. H); 6.78 (*s*, H–C(3)); 6.12 (*s*, H–C(9)); 6.04 (*s*, H–C(5)); 5.96 (*s*, H–C(7)); 3.86, 3.74 (2*s*, 2 MeOCO); 2.16 (*s*, Me–C(6)); 1.99 (*s*, Me–C(8)); 1.68 (*s*, Me–C(10)).

Data of **7b**. This form crystallized from the 77:23 equilibrium mixture in Et$_2$O/hexane in orange crystals. M.p. 171.3–172.1°. UV: See *Table 6* and *Fig. 11,f*. IR (KBr): 2950*w*, 1720*s*, 1700*s*, 1640*w*, 1600*w*, 1570*w*, 1490*w*, 1440*m*, 1430*s*, 1390*w*, 1370*w*, 1330*m*, 1310*m*, 1280*s*, 1230*s*, 1200*m*, 1190*m*, 1130*s*, 1050*m*, 1040*m*, 1000*w*, 960*w*, 930*w*, 920*w*, 880*w*, 850*w*, 810*w*, 780*m*, 770*m*, 740*m*, 700*m*. ^{1}H-NMR (300 MHz, CDCl$_3$, –20°): 7.88 (*s*, H–C(3)); 7.51–7.31 (*m*, 5 arom. H); 6.32 (*s*, H–C(1)); 6.19 (*s*, H–C(9)); 5.97 (*s*, H–C(7)); 3.75, 3.71 (2*s*, 2 MeOCO); 2.05 (*s*, Me–C(8)); 1.99 (*s*, Me–C(6)); 1.84 (*s*, Me–C(10)). ^{1}H-NOE (400 MHz, CDCl$_3$): 1.84 (Me–C(10))→6.19 (s, H–C(9)), 6.32 (s, H–C(1)); 2.05 (Me–C(8))→6.19 (s, H–C(9)), 5.97 (s, H–C(7)). EI-MS: 389 (16), 388 (100, *M*$^{+}$), 373 (11), 341 (23), 329 (28, [*M* – COOMe]$^+$), 297 (11), 286 (12, [*M* – PhC≡CH]$^+$), 269 (27), 255 (17), 254 (22), 253 (14), 252 (18), 247 (13), 246 (88, [*M* – E–C≡C–E]$^+$). Anal. calc. for C$_{25}$H$_{24}$O$_4$ (388.47): C 77.30, H 6.23; found: C 77.09, H 6.43.

The structure of **7b** was confirmed by an X-ray crystal-diffraction analysis (see *Tables 1* and *7* as well as *Fig. 2*).

3. *6,8,10-Trimethyl-5-[(E)-2-phenylethenyl]heptalene-1,2-dicarboxylate and 6,8,10-Trimethyl-1-[(E)-2-phenylethenyl]heptalene-4,5-dicarboxylate* (**11a** and **11b**, resp.). Synthesis and spectral characterization of **11b** were described in [24]. The X-ray crystal diffraction analysis of **11b** (see *Tables 1* and *7*, and *Fig. 3*) showed that the (*E*)-PhCH=CH substituent adopts an almost perfect s-*trans*-conformation with respect to the C(1)=C(2) bond of the heptalene skeleton (Θ(C(2')=C(1')–C(1)=C(2)) = 179.3(2)° (*cf. Table 1*). To establish the s-*trans*-conformation of **11b** also in solution (CDCl$_3$) the following ^{1}H-NOE measurements (400 MHz) were performed: 1.65 (Me–C(10))→6.94 (w; *d*, *J* = 15.8, H–C(1')), 6.37 (s; *d*, *J* = 15.8, H–C(2')), 6.24 (s, H–C(9)); integration of the *d* at 6.94 and 6.37 gave a ratio of *ca.* 1:3[23]). 2.12 (Me–C(8))[24]→6.24 (s, H–C(9)), 6.14 (s, H–C(7)); 6.55 H–C(2))→7.69 (s, H–C(3)), 6.94 (s, H–C(1')), no effect on H–C(2') at 6.37. UV of **11b**: See *Table 4* and *Fig. 8,b*.

Heating of **11b** at 60–80° did not lead to the formation of its DBS isomer **11a** (HPLC and ^{1}H-NMR; limit of detection of **11a** ≥ 0.5%). However, irradiation of **11b** in hexane with 366-nm light of a fluorescence tube established a photostationary state consisting of 68% of **11b** and 32% of **11a**. The photostationary state could be shifted to 20% of **11b** and 80% of **11a**, when the irradiation was performed through a cut-off filter of an aq. 1N NaNO$_2$ soln. (λ > 400 nm; *cf.* [59]) with a high-pressure Hg lamp. Heating of this soln. at 80° transformed **11a** again, quantitatively, into **11b**. ^{1}H-NMR (300 MHz, CDCl$_3$) of **11a**: 7.46–7.22 (*m*, 5 arom. H); 6.95 (*d*, *J*(3,4) = 12.0, H–C(4)); 6.82 (*d*, *J* = 16.3, PhCH=C*H*); 6.80 (*d*, *J*(4,3) = 12.0, H–C(3)); 6.58 (*d*, *J* = 16.3, PhC*H*=CH); 6.17 (*s*, H–C(9)); 6.13 (*s*, H–C(7)); 3.85, 3.78 (2*s*, 2 MeOCO); 2.23 (*s*, Me–C(6)); 2.05 (*s*, Me–C(8)); 1.75 (*s*, Me–C(10)). ^{1}H-NOE (400 MHz, CDCl$_3$): 2.13 (Me–C(6))→6.82 (s; *d*, *J* = 16.3, H–C(1')), 6.14 (s, H–C(7)); 6.58 (H–C(2'))→7.41 (m, 2 H$_o$ of Ph), 6.95 (s, H–C(4)); 6.95 (H–C(4))→6.80 (s, H–C(3)), 6.58 (s, H–C(2')). These results demonstrate that **11a** exists in solution almost exclusively in the s-*trans*-conformation with respect to its structural segment C(2')=C(1')–C(5)=C(5a). UV of **11a**: see *Table 4* and *Fig. 8,a*.

---

[23]) According to the X-ray crystal-structure analysis, H–C(1') and H–C(2') show shortest distances to the H-atoms of Me–C(10) of 324 and 237 ppm, respectively. If we take into account that the magnitude of the transfer of magnetization depends on the distance by $1/r^6$ (*cf.* [58]), H–C(1') and H–C(2') should exhibit in the s-*trans*-conformation of C(1')=C(2')–C(1)=C(2) an enhancement ratio of *ca.* 1:6, *i.e.*, quite close to the observed ratio of 1:3, when Me–C(10) is irradiated. This means that the observed ^{1}H-NOE on H–C(1') in **11b** is not attributable to the presence of a certain amount of the s-*cis*-conformer of **11b**.

[24]) This ^{1}H-NOE experiment shows that the chemical shifts of Me–C(8) and Me–C(6) (*i.e.*, Me–C(10) in [24]) have to be exchanged with respect to the assignments given in [24]. UV of **11b**: See *Table 4* and *Fig. 8,b*.

3.1. *(–)-(P)-* and *(+)-(M)-6,8,10-Trimethyl-5-[(E)-2-phenylethenyl]heptalene-1,2-dicarboxylate* ((–)-(P)-**11a** and (+)-(M)-**11a**, resp.). Irradiation of **11b** in hexane as described in *3* led to a photostationary state with 20% of **11b** and 80% of **11a**. Chromatography on the *Chiralcel OD* column with hexane/7% i-PrOH (flow rate 0.5 ml/min) resulted in a partial separation of (–)-(P)- and (+)-(M)-**11a** (separation factor 50%; t_R ((M)/(P)) = 1.03) and no separation of (–)-(P)- and (+)(M)-**11b** (t_R(MP)-**11b**/(P)-**11a**) = 1.27). Two consecutive separations of the 'photo'-mixture (1.8 mg) led to pure (–)-(P)- and (+)-(M)-**11a**. *CD of (–)-(P)-***11a** (hexane; extrema in mdeg): 500 (0), 400 (sh, –10.1), 350 (–17.1), 320 (0), 285 (100.3), 254 (0), 249 (–6.1), 244 (0), 237 (sh, 10.7), 233.5 (12.7), 226 (0), 213 (–31.5), 208 (0); see also *Fig.8,c*. *CD of (+)-(M)-***11a** (hexane; extrema in mdeg): 500 (2.8), 400 (sh, 12.4), 350 (19.1), 319 (0), 285 (–102.6), 255 (0), 249 (6.9), 245 (0), 238 (sh, 9.8), 234 (–11.9), 227 (0), 213 (36.0), 208 (0); see also *Fig.8,c*.

3.2. *(–)-(P)-* and *(+)-(M)-6,8,10-Trimethyl-1-[(E)-2-phenylethenyl]heptalene-4,5-dicarboxylate* ((–)-(P)-**11b** and (+)-(M)-**11b**, resp.). The probes of (–)-(P)-**11a** and (+)(M)-**11a** (see *3.1*) were dissolved in toluene (0.5 ml) and heated at 80°. Following the thermal isomerization with ·HPLC indicated that (–)-(P)-**11a** and (+)-(M)-**11a** gave within 1.75 h quantitatively (–)-(P)-**11b** and (+)-(M)-**11b**, respectively. *CD of (–)-(P)-***11b** (hexane; extrema in $\Delta\varepsilon$ with respect to $\varepsilon = 2.6915 \cdot 10^4\ 1\ mol^{-1}cm^{-1}$ at 321.2 nm of pure (MP)-**11b** in hexane): 550 (0), 402.6 (–42.70), 348.6 (0), 306.4 (50.60), 263.8 (min, 8.1), 251.6 (24.66), 2347.0 (min, 2.4), 222.2 (22.50), 210.6 (0); see also *Fig.8,d*. *CD of (+)-(M)-***11b** (hexane; extrema in $\Delta\varepsilon$): 550 (0), 401.6 (44.90), 348.4 (0), 306.4 (–52.81), 263.6 (max, –8.6), 251.4 (–25.70), 237.0 (max, –2.5), 221.2 (–23.37), 210.4 (0); see also *Fig.8,d*.

4. *5-[(E)-2-(4-Chlorophenyl)ethenyl]-6,8,10-trimethylheptalene-1,2-dicarboxylate and 1-[(E)-2-(4-Chlorophenyl)ethenyl]-6,8,10-trimethylheptalene-4,5-dicarboxylate* (**12a** and **12b**, resp.). Synthesis and spectral characterization of **12b**: see [24]. The chemical shifts for Me–C(8) and Me–C(6) (Me–C(10) in [24]) have to be exchanged. UV: see *Table 4* and *Fig.7,f*.

Irradiation of **12b** in hexane with 366-nm light of a fluorescence tube established rapidly a photostationary state consisting of 20% **12a** and 80% **12b**. UV of **12a**: see *Table 4* and *Fig.7,e*. ¹H-NMR (300 MHz, CDCl₃; in the presence of 80% of **12b**): 7.34–7.24 (*m*, 4 arom. H, 4-ClC₆H₄C*H*=CH); 6.90 (*d*, J(3,4) = 12.0, H–C(4)); 6.77 (*d*, J(4,3) = 120, H–C(3)); 6.19 (*s*, H–C(9)); 6.16 (*s*, H–C(7)); 3.85, 3.74 (2s, 2 MeOCO); 2.11 (*s*, Me–C(6)); 2.05 (*s*, Me–C(8)); 1.76 (*s*, Me–C(10)).

5. *5-[(E)-2-(4-Methoxyphenyl)ethenyl]-6,8,10-trimethylheptalene-1,2-dicarboxylate and 1-[(E)-2-(4-Methoxyphenyl)ethenyl]-6,8,10-trimethylheptalene-4,5-dicarboxylate* (**13a** and **13b**, resp.). Synthesis and spectral characterization of **13b**: see [24]. The chemical shifts for Me–C(8) and Me–C(6) (Me–C(10) in [24]) have to be exchanged. UV: see *Table 4* as well as *Fig.8,f*.

Irradiation of **13b** in hexane with 366-nm light of a fluorescence tube led to a photostationary state consisting of 87% of **13b** and 13% of **13a**. UV of **13a**: see *Table 4* and *Fig.8,e*. ¹H-NMR (300 MHz, CDCl₃; in the presence of 87% of **13b**): 7.36 (*d*, J = 8.2, 2 arom. H); 6.95 (*d*, J(3,4) = 11.9, H–C(4)); 6.87 (*d*, J = 8.2, 2 arom. H); 6.78 (*d*, J(4,3) = 11.9, H–C(3)); 6.69 (*d*, J = 16.3, 4-MeOC₆H₄CH=C*H*); 6.52 (*d*, J = 16.3, 4 MeOC₆H₄C*H*=CH); 6.16 (*s*, H–C(9)); 6.11 (*s*, H–C(7)); 3.85, 3.82 (2s, 2 MeOCO); 2.13 (*s*, Me–C(6)); 2.04 (*s*, Me–C(8)); 1.75 (*s*, Me–C(10)).

6. *5-(4-Methoxyphenyl)-6,8,10-trimethylheptalene-1,2-dicarboxylate and 1-(4-Methoxyphenyl)-6,8,10-trimethylheptalene-4,5-dicarboxylate* (**10a** and **10b**, resp.). 1-(4-Methoxyphenyl)-4,6,8-trimethylazulene (0.276 g; 1.00 mmol) [35], dimethyl acetylenedicarboxylate (0.426 g; 3.00 mmol), and [RuH₂(PPh₃)₄] (0.058 g; 0.05 mmol) were dissolved in MeCN (5 ml) and heated in a closed *Schlenk* tube at 110° for 24 h. The usual workup (*cf.* [24]) and chromatography on silica gel (hexane/Et₂O 7:3) led to four fractions containing *dimethyl (E)-1-[3-(4-methoxyphenyl)-4,6,8-trimethylazulen-1-yl]ethene-1,2-dicarboxylate* ((E)-**21**; 0.0084 g, 2%), *dimethyl 1-(4-methoxyphenyl)-5,6,8-trimethylacenaphthylene-3,4-dicarboxylate* (**22**; 0.0083 g, 2%), **10b** (0.0125 g, 3%), and *dimethyl 4,6,8-trimethylazulene-1,2-dicarboxylate* (0.152 g, 53%) [25].

*Data of (E)-***21**. brown crystals. M.p. 122.9–123.8° (Et₂O/hexane). IR (KBr): 3020w, 2980w, 2940w, 2820w, 1720s, 1710s, 1610s, 1570m, 1550w, 1525w, 1500s, 1430s, 1370m, 1315m, 1280s, 1240s, 1180s, 1170s, 1150s, 1110m, 1100w, 1060w, 1020s, 990w, 940w, 890w, 870w, 840w, 830m, 800w. ¹H-NMR (300 MHz, CDCl₃): 7.30 (*d*, J = 8.9, 2 arom. H); 7.06 (*s*, MeOCOC*H*=); 6.96 (*s*, H–C(7)); 6.93 (*d*, J = 8.9, 2 arom. H); 6.92 (*s*, H–C(5)); 6.90 (*s*, H–C(2)); 3.87 (*s*, MeO); 3.78, 3.51 (2s, 2 MeOCO); 2.75 (*s*, Me–C(8)); 2.55 (*s*, Me–C(6)); 2.42 (*s*, Me–C(4)). EI-MS: 419 (28), 418 (100, M^+), 404 (11), 403 (40), 359 (60, $[M – COOMe]^+$).

Data of **22**. Yellow crystals. M.p. 190.6–191.0 (Et₂O/hexane). IR (KBr): 2980w, 2940w, 2840w, 1740s, 1720s, 1610m, 1570w, 1540w, 1490m, 1450m, 1440m, 1430m, 1400m, 1370m, 1330w, 1280m, 1270s, 1240s, 1200s, 1180s, 1150m, 1110w, 1070w, 1050m, 1040m, 1030m, 990w, 970w, 900w, 870w, 840m, 820w, 800w. ¹H-NMR (300 MHz,

CDCl$_3$): 7.46 (*d*, *J* = 8.7, 2 arom. H); 7.13 (*s*, H–C(7) or H–C(2)); 7.11 (*s*, H–C(2) or H–C(7)); 6.99 (*d*, *J* = 8.7, 2 arom. H); 3.99, 3.97 (2*s*, 2 MeOCO); 3.89 (*s*, MeO); 2.83 (*s*, Me–C(5)); 2.80 (*s*, Me–C(6)); 2.31 (*s*, Me–C(8)). CI-MS (NH$_3$): 436 (7), 434 (7, [*M* + NH$_4$]$^+$), 419 (10), 418 (46), 417 (100, [*M* + 1]$^+$), 416 (21), 389 (7), 388 (23), 387 (86), 389 (28), 385 (93). Anal. calc. for C$_{26}$H$_{24}$O$_5$ (416.48): C 74.98, H 5.81; found: C 74.71, H 5.96.

Data of **10b**. Orange crystals. M.p. 169.5–170.0° (Et$_2$O/hexane). IR (KBr): 1720*s*, 1640*w*, 1600*w*, 1550*w*, 1500*s*, 1440*m*, 1380*w*, 1370*w*, 1300*m*, 1280*s*, 1250*s*, 1200*w*, 1180*s*, 1160*w*, 1110*w*, 1040*m*, 1030*w*, 820*w*, 780*w*. ^{1}H-NMR (300 MHz, CDCl$_3$): 7.73 (*d*, *J*(2,3) = 6.3, H–C(3)); 7.37 (*d*, *J* = 6.9, 2 arom. H); 6.88 (*d*, *J*(3,2) = 6.3, H–C(2)); 6.82 (*d*, *J* = 6.9, 2 arom. H); 6.20 (*s*, H–C(9)); 6.14 (*s*, H–C(7)); 3.80 (*s*, MeO); (3.75, 3.71 (2*s*, 2 MeOCO); 2.10 (*d*, *J*(7, Me–C(6)) = 1.1, Me–C(6)); 1.93 (*d*, *J*(9, Me–C(8)) = 1.1, Me–C(8)); 1.46 (*s*, Me–C(10)). EI-MS: 419 (31), 418 (100, *M*$^+$), 403 (10), 387 (10), 371 (13), 359 (14, [*M* – COOMe]$^+$), 327 (11, [*M* – COOMe – MeOH]$^+$), 300 (6), 286 (9, [*M* – 4-MeOC$_6$H$_4$C≡CH]$^+$), 285 (6), 277 (9), 276 (37, [*M* – E–C≡C–E]$^+$). UV: see *Table 4* as well as *Fig. 9, b*.

Heptalene **10b** in hexane did not give its DBS isomer **10a** on heating. However, on irradiation with 366-nm light of a fluorecence tube it easily rearranged to **10a** and formed a photostationary state which consisted of 62 % of **10b** and 38 % of **10a**. ^{1}H-NMR (300 MHz, CDCl$_3$) of **10a** (in the presence of 62 % of **10b**): 7.07 (*d*, *J* = 8.8, 2 arom. H); 6.83 (*m*, 2 arom. H, H–C(4)); 6.64 (*d*, *J*(4,3) = 11.9, H–C(3)); 6.24 (*s*, H–C(9)); 5.99 (*s*, H–C(7)); 3.87, 3.73 (2*s*, 2 MeOCO); 3.82 (*s*, MeO); 2.10 (*s*, Me–C(8)); 1.75 (*s*, Me–C(10)); 1.64 (*s*, Me–C(6)). UV: see *Table 4* and *Fig. 9, a*.

The structure of **10b** was confirmed by an X-ray crystal-diffraction analysis (see *Tables 1* and *7*, and *Fig. 4*).

7. *9-Isopropyl-6-methyl-1-[(E)-2-phenylethenyl]heptalene-4,5-dicarboxylate* (**16b**). Synthesis and spectral characterization: see [24]. UV: see *Table 5* and *Fig. 10, c*.

8. *9-Isopropyl-6-methyl-1-[(E)-2-(4-methoxyphenyl)ethenyl]heptalene-4,5-dicarboxylate* (**17b**). Synthesis and spectral characterization: see [24]. UV: see *Table 5* and *Fig. 10, d*.

9. *9-Isopropyl-1-methyl-6-[(E)-2-phenylethenyl]heptalene-4,5-dicarboxylate* (**18b**). Synthesis and spectral characterization: see [24]. UV: see *Table 5* as well as *Fig. 10, e*. The structure of **18b** was confirmed by an X-ray crystal-diffraction analysis (see *Tables 1* and *7*, and *Fig. 5*).

10. *9-Isopropyl-1-methyl-6-[(E)-2-(4-methoxyphenyl)ethenyl]heptalene-4,5-dicarboxylate* (**19b**). Synthesis and spectral characterization: see [24]. UV: see *Table 5* as well as *Fig. 10, f*.

Remarks on the Crystal-Structure Determinations[25]). – All measurements were conducted on a *Rigaku AFC5R* diffractometer fitted to a 12-kW rotating anode generator. The intensities were collected using *w*/2*q* scans and three standard reflections, which were measured after every 150 reflections, remained stable throughout each data collection. The intensities were corrected for *Lorentz* and polarization effects, and, except for **18b**, an empirical absorption correction [60] was applied. Each structure was solved by direct methods using SHELXS86 [61] which revealed the positions of all non-H-atoms. The non-H-atoms were refined anisotropically. The H-atoms were located in difference electron-density maps, and, with the exception of the Me H-atoms of **18b**, their positions were refined together with individual isotropic displacement parameters. The Me H-atoms of **18b** were fixed in geometrically idealized positions (*d*(C–H) = 0.95 Å), and their isotropic displacement parameters were allowed to refine. A correction for secondary extinction was applied for **8b** and **18b**. All refinements were carried out on *F* using full-matrix least-squares procedures which minimized the function $Sw(|F_o| – |F_c|)^2$, where $1/w = [s^2(F_o) + (pF_o)^2]$. The data collection and refinement parameters for each compound are listed in *Table 7*. Neutral atom scattering factors for non-H-atoms were taken from [62a] (from [63a] for **8b** and **18b**) and the scattering factors for H-atoms from [64]. Anomalous dispersion effects were included in F_c [65]; the value for *f'* and *f''* were taken from [62b] (from [63b] for **8b** and **18b**). All calculations were performed using the TEXSAN [66] crystallographic software package and the figures wer produced with ORTEPII [67].

One ester group in **11b** is disordered with the C=O and Me groups exchanging places in 17 % of the molecule. Two positions were defined for the Me group, but it was not possible to refine separate positions for the disordered O-atoms. H-Atoms were not included for the minor orientation of the Me group.

---

[25]) Crystallographic data (excluding structure factors) for the structures reported in this paper have been deposited with the *Cambridge Crystallographic Data Centre* as supplementary publication No. CCDC-10/29. Copies of the data can be obtained, free of charge, on application to the Director, CCDC, 12 Union Road, Cambridge CB2 1 EZ, UK. (fax: +44(0)1223336033 or email: teched @ chemcrys.cam.ac.uk).

Table 7. *Crystallographic Data for Dimethyl Heptalene-4,5-dicarboxylates*

	8b	7b	11b	10b	18b
Crystallized from	Et_2O/hexane	Et_2O/hexane	Et_2O/hexane	Et_2O/hexane	Et_2O/hexane
Empirical formula	$C_{27}H_{26}O_4$	$C_{25}H_{24}O_4$	$C_{27}H_{26}O_4$	$C_{26}H_{26}O_5$	$C_{28}H_{28}O_4$
Formula weight	414.50	388.46	414.50	418.49	428.53
Crystal color, habit	orange-red, plate	orange, prism	orange, plate	orange, prism	orange, prism
Crystal dimensions [mm]	$0.10 \times 0.30 \times 0.33$	$0.18 \times 0.22 \times 0.45$	$0.08 \times 0.40 \times 0.45$	$0.21 \times 0.33 \times 0.48$	$0.23 \times 0.28 \times 0.30$
Crystal temp. [K]	173 (1)	173 (1)	173 (1)	173 (1)	296 (1)
Radiation, wavelength [Å]	MoK_α, 0.71069	MoK_α, 0.71069	MoK_α, 0.71069	MoK_α, 0.71069	CuK_α, 1.54179
Crystal system	monoclinic	triclinic	monoclinic	triclinic	monoclinic
Lattice parameters					
Reflections for cell determination	23	25	25	22	23
2θ range [°]	21–38	37–40	30–40	39–40	93–96
a [Å]	8.140 (2)	10.133 (3)	13.305 (2)	11.147 (2)	9.511 (2)
b [Å]	12.098 (2)	11.756 (3)	9.633 (3)	14.128 (6)	16.913 (2)
c [Å]	22.327 (3)	9.843 (3)	18.012 (3)	7.001 (4)	14.910 (2)
α [°]	90	110.02 (2)	90	97.64(4)	90
β [°]	94.87 (1)	107.74 (2)	104.05 (1)	99.84 (3)	91.25 (2)
γ [°]	90	99.20 (2)	90	93.95 (2)	90
V [Å³]	2190.8 (6)	1002.6 (5)	2239.5 (9)	1071.9 (8)	2397.9 (6)
Space group	$P2_1/n$	$P\bar{1}$ (# 2)	$P2_1/c$ (# 14)	$P\bar{1}$	$P2_1/n$
Z	4	2	4	2	4
D_x [g cm⁻³]	1.257	1.287	1.229	1.296	1.187
μ [mm⁻¹]	0.0778	0.0800	0.0760	0.0890	0.592
Absorption correction (min; max)	0.770; 1.289	0.874; 1.136	0.778; 1.119	0.818; 1.115	–
$2\theta_{(max)}$ [°]	60	60	60	60	120
Total reflections measured	7105	6130	7154	6516	3977
Symmetry-independent reflections	6685	5827	6526	6220	3728
Reflections used [$I > 3\sigma(I)$]	3210	4397	4015	4416	3088
Variables	385	358	394	384	357
Final R	0.0478	0.0389	0.0461	0.0375	0.0397
R_w	0.0420	0.0386	0.0427	0.0383	0.0450
p for $1/w = [\sigma^2(F_o) + (pF_o)^2]$	0.0025	0.005	0.005	0.008	0.005
Goodness of fit s	1.682	1.888	1.651	1.802	3.324
Secondary extinction coefficient	1.13×10^{-7}	–	–	–	2.41×10^{-6}
Final Δ_{max}/σ	0.005	0.0005	0.0003	0.0005	0.0001
$\Delta\rho$ (max; min) [e Å⁻³]	0.28; −0.20	0.24; −0.19	0.34; −0.30	0.25; −0.17	0.14; −0.16

REFERENCES

[1] a) W. Bernhard, P.Brügger, P. Schönholzer, R.H. Weber, H.-J. Hansen, *Helv. Chim. Acta* **1985**, *68*, 429; b) R.H. Weber, P. Brügger, T.A. Jenny, H.-J. Hansen, *ibid.* **1987**, *70*, 742.

[2] K. Hafner, G.L. Knaup, H.J. Lindner, *Bull. Chem. Soc. Jpn.* **1988**, *61*, 155.

[3] L.A. Paquette, *Pure App. Chem.* **1982**, *54*, 987.

[4] K. Hafner, G.L. Knaup, H.J. Lindner, H.-C. Flöter, *Angew. Chem.* **1985**, *97*, 209; *ibid. Int. Ed.* **1985**, *24*, 212.

[5] a) F.A.L. Anet, L.A. Bock, *J. Am. Chem. Soc.* **1968**, *90*, 7130; b) L.A. Paquette, J.M. Photis, G.D. Ewing, *ibid.* **1975**, *97*, 2538.

[6] a) L.A. Paquette, T.-Z. Wang, J. Luo, Ch. E. Cottrell, A.E. Clough, L.B. Anderson, *J. Am. Chem. Soc.* **1990**, *112*, 239; b) L.A. Paquette, M.P. Trova, J. Luo, A.E. Clough, L.B. Anderson, *ibid.* **1990**, *112*, 228.

[7] A Guide to IUPAC Nomenclature of Organic Compounds, Recommendations 1993, prepd. for publ. by R. Panico, W.H. Powell, and J.-C. Richter, Blackwell Scientific Publications, Oxford, 1993, p. 47.

[8] L.A. Paquette, J.M. Gardlik, L.K. Johnson, K.J. McCullough, *J. Am. Chem. Soc.* **1980**, *102*, 5026.

[9] J.M. Gardlik, L.A. Paquette, R. Gleiter, *J. Am. Chem. Soc.* **1979**, *101*, 1617; L.A. Paquette, J.M. Gardlik, *ibid.* **1980**, *102*, 5016.

[10] L.A. Paquette, Y. Hanzawa, G.-J. Hefferon, J.F. Blount, *J. Org. Chem.* **1982**, *47*, 265.

[11] W. Bernhard, P. Brügger, J.J. Daly, G. Englert, P. Schönholzer, H.-J. Hansen, *Helv. Chim. Acta* **1985**, *68*, 1010.

[12] K. Hafner, G.L. Knaup, *Tetrahedron Lett.* **1986**, *27*, 1673.

[13] Y. Chen, Ph.D. thesis, University of Zurich, 1992.

[14] L.A. Paquette, J.M. Photis, *J. Am. Chem. Soc.* **1976**, *98*, 4936.

[15] R. Huisgen, F. Mietzsch, *Angew. Chem.* **1964**, *76*, 36; *ibid. Int. Ed.* **1964**, *3*, 83.

[16] P. Uebelhart, H.-J. Hansen, unpublished results.

[17] Y. Chen, R.W. Kunz, P. Uebelhart, R.H. Weber, H.-J. Hansen, *Helv. Chim. Acta* **1992**, *75*, 2447.

[18] A. Streitwieser, Jr., 'Molecular Orbital Theory for Organic Chemists', John Wiley & Sons, Inc., New York–London, 1961, p. 16ff.

[19] J. Stegemann, H.J. Lindner, *Tetrahedron Lett.* **1977**, 2515.

[20] H.J. Lindner, B. Kitschke, *Angew. Chem.* **1976**, *88*, 123; *ibid. Int. Ed.* **1976**, *15*, 106.

[21] J. Bordner, R.G. Parker, R.H. Stanford, Jr., *Acta Crystallogr., Sect. B* **1972**, *28*, 1969; H. Quast, T. Herkert, A. Witzel, E.M. Peters, K. Peters, H.G. von Schnering, *Chem. Ber.* **1994**, *127*, 921.

[22] K.H. Claus, C. Kruger, *Acta Crystallogr., Sect. C* **1988**, *44*, 1632.

[23] K. Hafner, H. Diehl, H.U. Süss, *Angew. Chem.* **1976**, *88*, 121; *ibid. Int. Ed.* **1976**, *15*, 104.

[24] A.A.S. Briquet, H.-J. Hansen, *Helv. Chim. Acta* **1994**, *77*, 1940.

[25] W. Bernhard, P. Brügger, J.J. Daly, P. Schönholzer, R.H. Weber, H.-J. Hansen, *Helv. Chim. Acta* **1985**, *68*, 415.

[26] W. Bernhard, H.-R. Zumbrunnen, H.-J. Hansen, *Chimia* **1979**, *33*, 324.

[27] R.H. Weber, Ph.D. thesis, University of Basel, 1988.

[28] Yu. A. Ustynyuk, O.I. Trifonova, A.V. Yatsenko, A.A. Borisenko, H.-J. Hansen, P. Uebelhart, *Russ. Chem. Bull.* **1994**, *43*, 2100.

[29] A. Ehmann, R. Gompper, H. Hartmann, T.J.J. Müller, K. Polborn, R. Schütz, *Angew. Chem.* **1994**, *106*, 581; *ibid. Int. Ed.* **1994**, *33*, 572; R.H. Berg, S. Hvilsted, P.S. Ramanujam, *Nature (London)* **1996**, *383*, 505.

[30] A.J. Rippert, H.-J. Hansen, *Helv. Chim. Acta* **1995**, *78*, 238.

[31] A.A.S. Briquet, H.-J. Hansen, *Helv. Chim. Acta* **1994**, *77*, 1921.

[32] M. Head-Gordon, J.A. Pople, *J. Phys. Chem.* **1993**, *97*, 1147.

[33] O. Lhost, J.L. Brédas, *J. Chem. Phys.* **1992**, *96*, 5279.

[34] M. Traetteberg, E.B. Frantsen, F.C. Mijlhoff, A. Hoekstra, *J. Mol. Struct.* **1975**, *26*, 57.

[35] A.A.S. Briquet, H.-J. Hansen, *Helv. Chim. Acta* **1994**, *77*, 1577.

[36] A. Linden, M. Meyer, P. Mohler, A.J. Rippert, H.-J. Hansen, *Helv. Chim. Acta* **1997**, *80*, in preparation.

[37] A.J. Rippert, H.-J. Hansen, *Helv. Chim. Acta* **1997**, *80*, in preparation.

[38] P. Uebelhart, H.-J. Hansen, *Helv. Chim. Acta* **1992**, *75*, 2493.

[39] H.J. Dauben, Jr., D.J. Bertelli, *J. Am. Chem. Soc.* **1961**, *83*, 4659.

[40] E. Vogel, H. Königshofen, J. Wassen, K. Müllen, J.F.M. Oth, *Angew. Chem.* **1974**, *86*, 777; *ibid. Int. Ed.* **1974**, *13*, 732.

[41] J. Wassen, Ph.D. thesis, University of Cologne, 1977.

[42] E. Vogel, H. Königshofen, K. Müllen, J.F.M. Oth, *Angew. Chem.* **1974**, *86*, 229; *ibid. Int. Ed.* **1974**, *13*, 281; H. Königshofen, Ph.D. thesis, University of Cologne, 1973.

[43] E. Vogel, H. Hogrefe, *Angew. Chem.* **1974**, *86*, 779; *ibid. Int. Ed.* **1974**, *13*, 735.
[44] M. Kataoka, T. Nakajima, *Bull. Chem. Soc. Jpn.* **1992**, *65*, 2371.
[45] M. Kataoka, T. Ohmae, T. Nakajima, *J. Org. Chem.* **1986**, *51*, 358.
[46] H.-J. Hansen, unpublished results.
[47] P. Kouroupis, H.-J. Hansen, *Helv. Chim. Acta* **1995**, *78*, 1247.
[48] P. Uebelhart, P. Mohler, R.-A. Fallahpour, H.-J. Hansen, *Helv. Chim. Acta* **1995**, *78*, 1437.
[49] U. Höweler, P. S. Chatterjee, K. A. Klingensmith, J. Waluk, J. Michl, *Pure Appl. Chem.* **1989**, *61*, 2117.
[50] T. Nakajima, *Topics Curr. Chem.* **1972**, *32*, 1.
[51] M. Kataoka, S. Noseki, T. Nakajima, *Nouv. J. Chim.* **1985**, *9*, 135.
[52] G. Buemi, F. Zuccarello, *Gazz. Chim. Ital.* **1985**, *115*, 103.
[53] J. Veciana, M. I. Crespo, *Angew. Chem.* **1991**, *103*, 85 (222); *ibid. Int. Ed.* **1991**, *30*, 74 (216).
[54] W. Hug, I. Tinoco, Jr., *J. Am. Chem. Soc.* **1973**, *95*, 2803.
[55] G. Gottarelli, H.-J. Hansen, G. P. Spada, R. H. Weber, *Helv. Chim. Acta* **1987**, *70*, 430.
[56] S. El Houar, H.-J. Hansen, *Helv. Chim. Acta* **1997**, *80*, in press.
[57] S. El Houar, H.-J. Hansen, *Chimia* **1996**, *50*, 341.
[58] D. Neuhaus, M. P. Williamson, 'The Nuclear Overhauser Effect in Structural and Conformational Analysis', VCH Publishers, Inc., New York, 1989.
[59] J. G. Calvert, J. N. Pitts, Jr., 'Photochemistry', John Wiley & Sons, Inc., New York, 1966, p. 737.
[60] N. Walker, D. Stuart, *Acta Crystallogr., Sect. A.* **1983**, *39*, 158.
[61] G. M. Sheldrick, SHELXS86. *Acta Crystallogr., Sect. A* **1990**, *46*, 467.
[62] a) E. N. Maslen, A. G. Fox, M. A. O'Keefe, in 'International Tables for Crystallography', Vol. C, Ed. A. J. C. Wilson, Kluwer Academic Publishers, Dordrecht, 1992; Table 6.1.1.1, pp. 477–486; b) D. C. Creagh, W. J. McAuley, *ibid.*, Table 4.2.6.8, pp. 219–222.
[63] a) D. T. Cromer, J. T. Waber, in 'International Tables for X-Ray Crystallography', Vol. IV, Eds. J. A. Ibers and W. C. Hamilton, The Kynoch Press, Birmingham, England, 1974, Table 2.2A, pp. 71–98; b) D. T. Cromer, J. A. Ibers, *ibid.*, Table 2.3.1, pp. 149–150.
[64] R. F. Stewart, E. R. Davidson, W. T. Simpson, *J. Chem. Phys.* **1965**, *42*, 3175.
[65] J. A. Ibers, W. C. Hamilton, *Acta Crystallogr.* **1964**, *17*, 781.
[66] TEXSAN. Single Crystal Structure Analysis Software, Version 5.0. Molecular Structure Corporation, The Woodlands, Texas, 1989.
[67] C. K. Johnson, ORTEPII. Report ORNL-5138, Oak Ridge National Laboratory, Oak Ridge, Tennessee 1976.